

Proyecto Final de Máster en Química Sostenible

Controllable Synthesis of Metal Nanoparticles for Catalytic Applications

Presentado por:

Lichen Liu

Dirigido por:

Prof. Avelino Corma



INSTITUTO DE
TECNOLOGÍA
QUÍMICA



CSIC
CONSEJO SUPERIOR DE INVESTIGACIONES CIENTÍFICAS



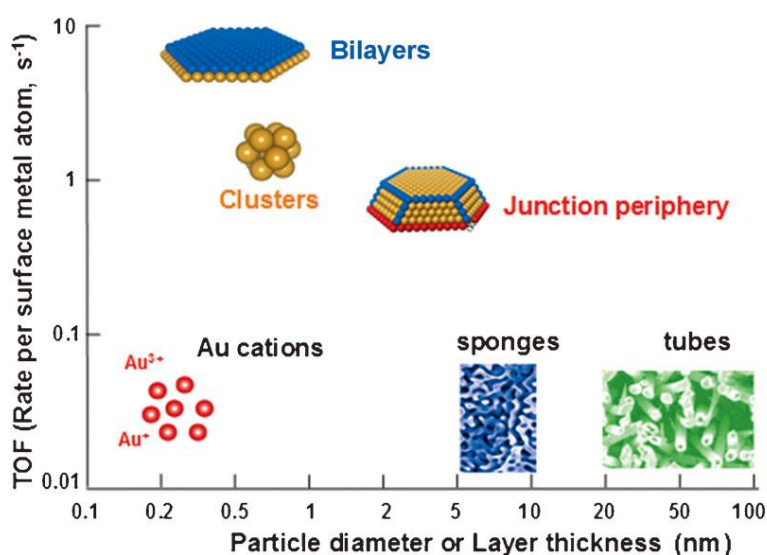
UNIVERSITAT
POLITÈCNICA
DE VALÈNCIA

1. Introduction	
1.1 Metal clusters: an emerging field in catalysis.....	2
1.2 Cu nanoparticles for C-N coupling reaction.....	4
1.3 Stabilizing metal nanoparticles by porous materials.....	11
2. Synthesis of Cu nanoparticles and catalytic properties in C-N coupling reaction	
2.1 Preparation of Cu nanoparticles (NPs).....	16
2.2 C-N coupling reaction activities.....	17
2.3 Conclusions.....	22
3. Ultra-small Pt nanoparticles confined in MCM-22	
3.1 Experimental details of synthesis.....	23
3.2 Results and discuss.....	24
3.3 Conclusions.....	27
4. Perspectives	

1. Introduction

1.1 Metal clusters: an emerging field in catalysis

Metal nanoparticles (NPs) are widely used catalysts in both fundamental research and industrial applications.¹ The catalytic properties of metal nanoparticles have been deeply investigated and many factors can have influences on their catalytic performances, including size, chemical components, surface structures, coordination environments, interactions between metal NPs and supports etc. Among these factors, the size effects on the catalytic properties are the most apparent factor. Lots of works have proved that controlling the particle size can be an effective strategy to modify the catalytic performances, but the relationships between particle sizes and activities are still not fully revealed due to the complexities of heterogeneous catalysts and the catalytic processes. Thanks to the developments of methodologies in catalyst synthesis and instruments for catalyst characterizations, we are continually approaching to understanding the active sites of metal NPs and relationships between the size and activity.



Scheme. 1 Turnover frequency of CO oxidation at room temperature for various states of gold.

In the past several decades, Au NPs have attracted great attention because of their superior activities in many reactions and fundamental significances in catalytic research. The dramatic discrepancies between nano-sized Au and bulk Au fascinate researchers to figure out the origins of the high activities of nano-sized Au. The activities of different Au species are listed in **Scheme 1**.² Firstly, based on results from TEM and FT-IR, Haruta et al. proposed that Au NPs with a diameter of ~2 nm are the active components.³ Subsequently, the interface between Au and the oxides supports are also thought important in the catalytic processes. Goodman et al. came up with further insights on the structures of active gold catalysts through surface science studies.⁴ They found that two-layer

Au is the most active structure in CO oxidation because of the transition from metallic to non-metallic.⁵ The great changes in electronic structures are the reasons accounting for the dramatic transformation of catalytic activities.⁶ Nevertheless, another viewpoint was come up by Hutchings and his co-workers. With the help of aberration-corrected TEM and STEM, they found that supported Au clusters with several Au atoms are the active species.⁷ The sub-nanoscale Au species are not studied systematically due to the limitation of TEM.

Although agreements have not been reached in the catalytic mechanisms of Au NPs, the Au species with sub-nanoscale sizes become a rising star in this field. In recent years, the structures and properties of Au clusters are reported both in experimental and theoretical aspects. Moreover, more and more researchers pay their attention to other metal NPs with sub-nanometer sizes. Lots of interesting and significant works have been done, which show us that the novel properties and promising applications of metal clusters. However, so far, there is still a unified definition of “cluster”. Generally, metal NPs smaller than 1 nm or with less than 20 atoms can be called cluster. Especially, clusters with several atoms or tens of atoms will show more distinct properties compared with metal NPs because of their unique electronic structures and geometric structures.

Actually, the physical and chemical properties are hot research topics in the 1980s and 1990s. Great progresses have been made in this field, especially in the physical properties of clusters. The geometric and electronic structures of metal clusters can be well described using theoretical physical models. Furthermore, on experimental aspect, the magnetic, optical and other properties of metal clusters are also investigated intensively. The catalytic properties of metal clusters have also attracted some attention. Metal clusters prepared through size-selected method show size-dependent activities, which can be ascribed to their different electronic structures. However, relationships between catalytic properties and structures of metal clusters are not well investigated, which may be caused by the limitations of characterizations and people’s understanding of catalysis. Nevertheless, the research interests seem to cool down in the end of 1990s, probably because people turn their attention to nanomaterials in the scale of 1~100 nm.

After synthesizing nanostructured metal-based catalysts with different morphologies and components and study their structure-activity relationships, we recognize that the structural factors in the nanoscale may not be the essential origins that affecting the catalytic properties. Catalytic reactions occur in the scale of angstrom (10^{-10} m), while the nanostructured materials usually in the scale of several or tens of nanometers (10^{-9} - 10^{-8} m). This nonidentity in scale may stunt our approach to the molecular and atomic understanding of catalysis. Coincidentally, clusters are species in the sub-nanometric scale, which can be matched with molecules. More importantly, as we just discussed

in the history of catalysis based on Au NPs, more and more facts imply that metal clusters can be the “actual” active species in many heterogeneous catalytic reactions. Therefore, in recent years, people’s interests are turned back to metal clusters. Based on previous achievements, new methods and advanced instruments are applied in this field, resulting in the fast developments both on theoretical and experimental aspects. Catalysis based on metal clusters is becoming an emerging field in catalysis, producing new concepts, methods and better catalysts.

1.2 Cu nanoparticles for C-N coupling reaction

Metal-catalyzed Coupling reactions (C-C, C-O, C-N etc.) have been hot research topics in recent years because these reactions are very important in organic synthesis. Based on coupling reactions, some complex compounds can be obtained through fewer steps compared with conventional methods. Pd and Cu are widely used in coupling reactions because of their good activity and wide reaction scopes. The Nobel award of chemistry in 2010 is given to three chemists because of their contributions in Pd-catalyzed cross coupling reactions.^{8,9} For Cu, because of its low cost and easy availability, Cu-catalyzed coupling reactions have received tremendous attention in organic synthesis. Actually, Cu-catalyzed coupling reactions have been applied to industrial applications long time ago.¹⁰ C-X coupling reactions using Cu-based catalysts are widely studied in recent years since the discovery of the application of diamine ligands that enabling the coupling of aryl halides and amides (the Goldberg reaction) to be performed under much milder conditions.¹¹ Since then, Cu-based catalysts for C-X coupling reactions have attracted much attention due to the wide scope of C-X coupling reactions when we use Cu-based catalysts.

In this part, we are focused on C-N coupling reaction. Compared with C-C coupling reactions, the construction of the C-N bonds of aromatic compounds is particularly important and proved to be challenging to medicinal chemists.¹² Furthermore, the Cu-based catalysts in this part is focused on Cu-based nanoparticles (Cu-based NPs, including Cu⁰, Cu₂O and CuO), which can be seen as “heterogeneous” catalysts compared with conventional Cu compounds as catalysts. Considering the different chemical states of Cu-based NPs and the effects of particle size and surface properties, the catalytic properties of Cu-based NPs will be more complicated. In recent years, there are a lot of progresses that have been made in this field. Herein, we will discuss the scope of reaction using Cu-based NPs in C-N coupling and the possible active species in these reactions. Considering the important effects of preparing method on the catalytic performances on Cu-based NPs, we will also discuss the relationships between preparing method and their catalytic properties.

1.2.1 Three-component condensation

Among the different multicomponent reactions, the catalytic coupling reaction of aldehyde, amine and alkyne (so-called A³ coupling) is one of the best examples, where propargylamines are produced as the main product. According to the work of Kidwai et al., Cu NPs seems the best compared with Ni, Ag and Au.¹³ The proposed reaction mechanism is also shown in Fig. 1. The activation of alkyne on Cu⁰ NPs is the key step. But these Cu NPs will gradually lose the activity after several cycles. Not only monodispersed Cu NPs, Cu NPs supported on TiO₂ can also show good activity in A³ coupling reaction.¹⁴ Similar results are also reported by using Cu⁰ NPs supported on montmorillonite.¹⁵ In their work, a small amount of CuO can be found in XRD, suggesting that the transformation of Cu(0) to Cu(II). Although heterogeneous Cu catalysts are active for this reaction, their real active species are not revealed based on their experimental results.

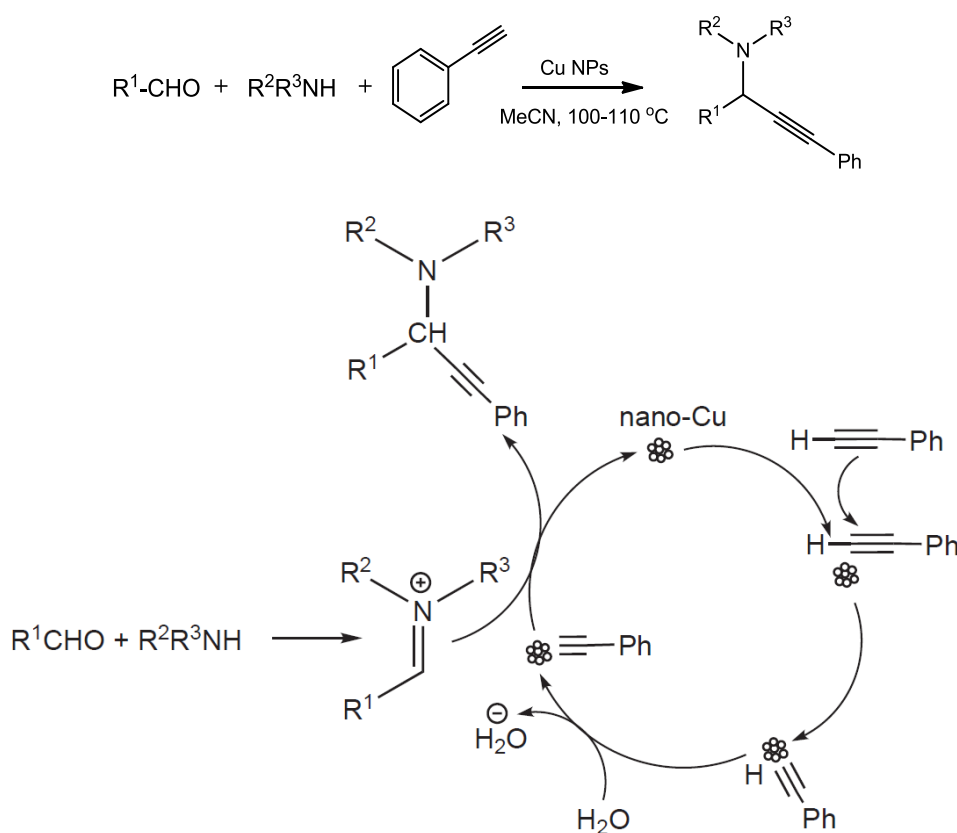
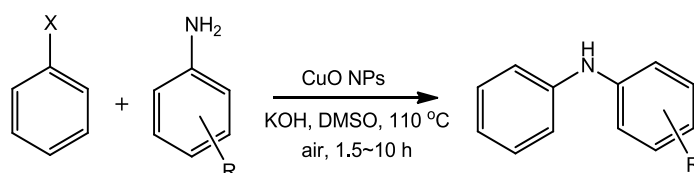


Fig. 1 A³ coupling reaction and the proposed mechanism

1.2.2 N-Arylation reaction



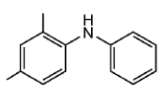
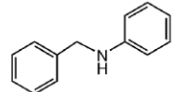
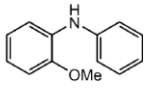
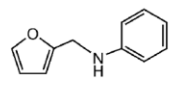
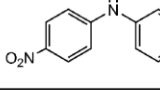
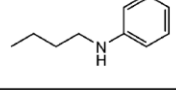
Product	Yield [%]	Product	Yield [%]
	92		90
	98		85
	70		91
[a] Reagents and reaction conditions: Aniline (2.5 mmol), iodobenzene (2 mmol), CuO NPs (1.2 mol%), KOH (2 mmol), DMSO (4 mL); 110 °C, air.			

Fig. 2 N-Arylation reaction catalyzed by CuO nanoparticles.

N-Arylation of amines through C-N cross-coupling reaction with aryl halides is a useful process for preparing aryl amines. For this reaction, almost stoichiometric amounts of Cu compounds are need in conventional procedures. Recently, Punniyamurthy *et al.* reported that CuO NPs can be used for the N-Arylation reactions under mild conditions with catalytic amount of Cu.¹⁶ In their work, the less active chlorobenzenes can also be activated by CuO nanoparticles. Besides, they also show that CuO NPs are quite stable for C-N coupling reactions after several cycles. TEM images of CuO NPs after three cycles are similar compared with the fresh CuO NPs.¹⁷ In addition, arylation of aromatic heterocycles can also be catalyzed by Cu₂O NPs. In the work of Li *et al.*, they developed a procedure based on Cu₂O NPs for N-arylation of nitrogen-containing heterocycles.¹⁸ Cu₂O NPs with different shapes are used for this reaction. Cubic NPs with {100} facets exposed show the best activity compared with bulky, octahedral, and spherical nanoparticles. Arylation of amides has also been realized by Cu-based NPs. For instance, Cu₂O nanoparticles in polyethylene glycol (PEG) are efficient and recyclable catalysts for the amidation of aryl iodides (**Fig. 4**).¹⁹ No ligand, additive, or cocatalyst is required for this reaction. However, this reaction can only activate aryl iodides, which are very expensive. To overcome this disadvantage, and his co-workers introduce diamine ligands (dimethylethylenediamine (DMEDA)) to improve the activity of Cu₂O NPs.²⁰ In that work, the less active aryl bromides and chlorides can be activate in high yields. But, the reason about the improvement effect of diamine ligands are not clearly explained in this paper. After introduction of diamine ligands, small Cu species (clusters?) may leach from Cu₂O NPs. In another work of Sreedhar *et al.*, they found that CuI NPs (about ~50 nm) are quite active for the activation of aryl chlorides in C-N coupling and C-O coupling reactions.²¹ But the question is, is CuI stable in DMF during the reaction because CuI can be soluble in DMF? In this short communication, they didn't do

many discussions on it although they show that the XRD patterns of fresh and used CuI NPs are almost the same except for the growth of the particle size.

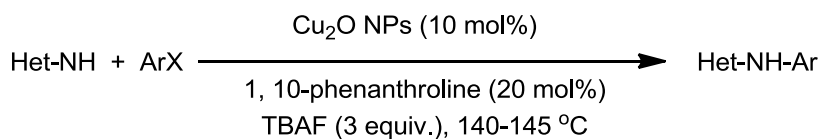


Fig. 3 N-arylation of N-containing aromatic heterocycle.

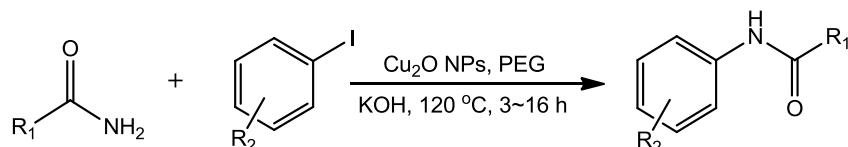


Fig. 4 Arylation of amides using aryl iodide.

1.2.3 Intramolecular C-N bond formation

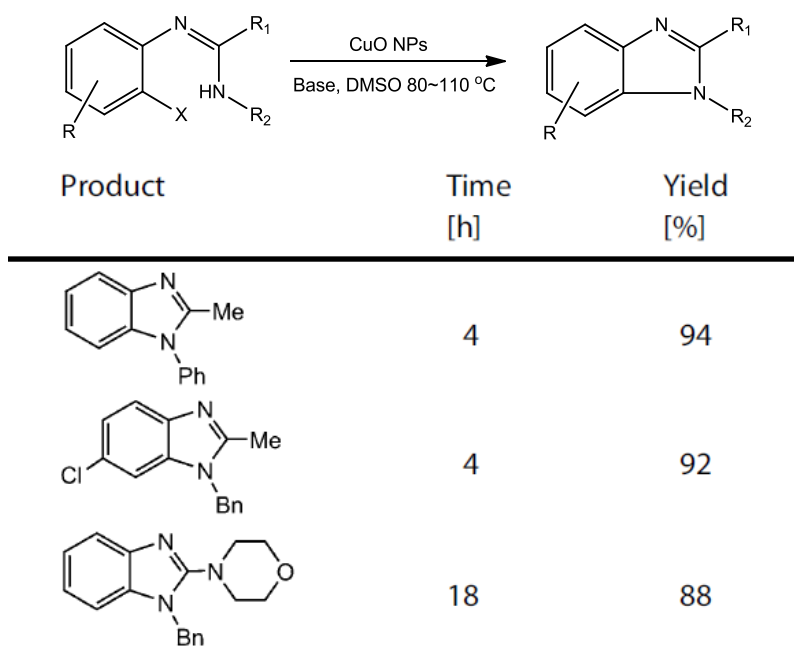


Fig. 5 CuO nanoparticle-catalyzed synthesis of substituted benzimidazoles

Using Cu-based NPs, we can also perform intramolecular C-N coupling reactions. A typical example is the synthesis of benzimidazole moieties, as shown in **Fig. 5**. Using this method, they can synthesize substituted benzimidazoles with compatibility with a variety of functional groups.²² In this paper, the authors also study the reaction mechanism of CuO NPs. The design such an experiment: the CuO nanoparticles were stirred at the reaction temperature (110 °C) for 10 h in the presence of K₂CO₃ in DMSO. The solution was then cooled to room temperature and subjected to

centrifugation. The particles were recovered and the clear solution was investigated for the cyclization of obromophenylbenzamide in the presence of fresh K_2CO_3 . No conversion can be detected. However, this experiment is not quite convincing because no reactant is added. The leaching of CuO may be caused by the interaction between heterogeneous CuO NPs and the reactants. Although the leaching amount of Cu salts in the solution is quite low, the real active species in this system is still not clear.

1.2.4 Aziridination reaction

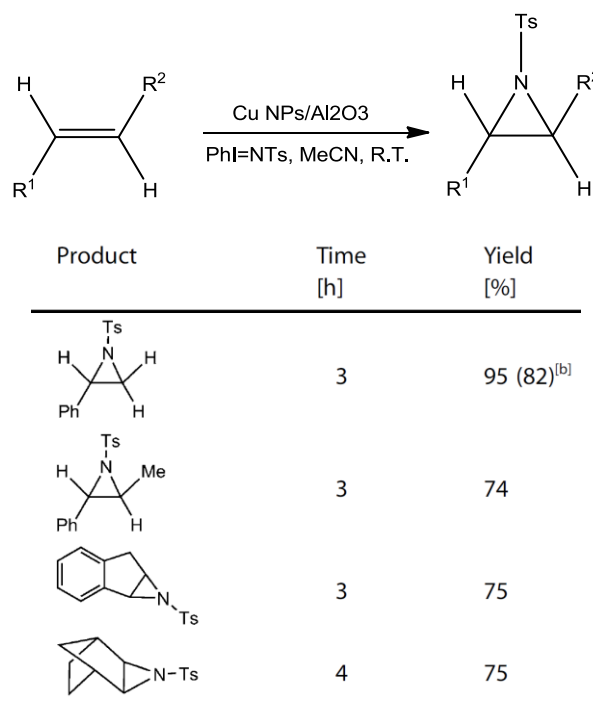


Fig. 6 Aziridination reactions catalyzed by Cu NPs supported on Al_2O_3 .

Recently, Kantam et al. reported an aziridination reaction (**Fig. 6**) catalyzed by alumina-supported Cu nanoparticles in moderate to high yields.^{23,24} In their works, Cu NPs supported on Al_2O_3 are prepared by aerogel method. From the XRD pattern, we can see a small peak corresponding to Cu_2O , suggesting that the surface of these Cu NPs should be partially oxidized. The triazole formation is achieved at room temperature in water. To test that if the reaction is heterogeneous or homogeneous, they perform a hot filtrate. No reaction activity is observed after remove the Cu- Al_2O_3 . They also test the recyclability of the catalyst. After 3 cycles, the catalyst is still stable without loss of activity.

1.2.5 Click reaction

Click chemistry is a newer approach to the synthesis of drug like molecules that can accelerate the drug discovery process by utilizing practical and reliable reactions. Sharpless and co-workers defined a click reaction as one that is wide in scope and easy to perform, uses readily available reagents, and

is insensitive to oxygen and water.^{25,26} A typical click chemistry example is the 1,3-dipolar Huisgen cycloaddition reaction (**Fig. 7**). Sharghi et al. developed a simple one-pot procedure for the synthesis of 1,2,3-triazole derivatives through a three-component coupling reaction using terminal alkynes, benzyl or alkyl halides, and sodium azide in the presence of 1 mol% Cu/CuI nanoparticles supported on carbon.²⁷ Both XRD peaks corresponding to Cu and CuI can be observed in this sample. The size of CuI particles are very large, as large as 2 μm . Cu species supported on activated charcoal offers superior catalytic activity and 1,4-regioselectivity towards the [3+2] Huisgen cycloaddition in water.²⁸ However, in this paper, $\text{Cu}(\text{NO}_3)_2$ was loaded on activated charcoal through impregnation method. Both Cu(I) and Cu(II) will be present in the Cu/C sample. The author only analyzed the content of Cu species in the products while not analyze the content of Cu species in the reaction mixture. Although they declared that this reaction should be a heterogeneous process, their proof was not solid enough. From the above two papers we can see that, organic chemists seem to haven't a clear concept on the definition of nanoparticles. They haven't performed correct characterizations on the structures of their catalysts. This seems a common problem for those who are focused on organic reactions.

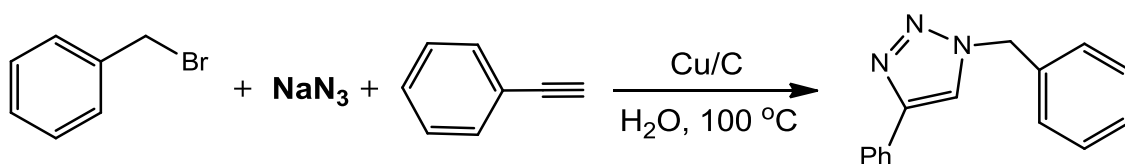


Fig. 7 1,3-dipolar Huisgen cycloaddition reaction.

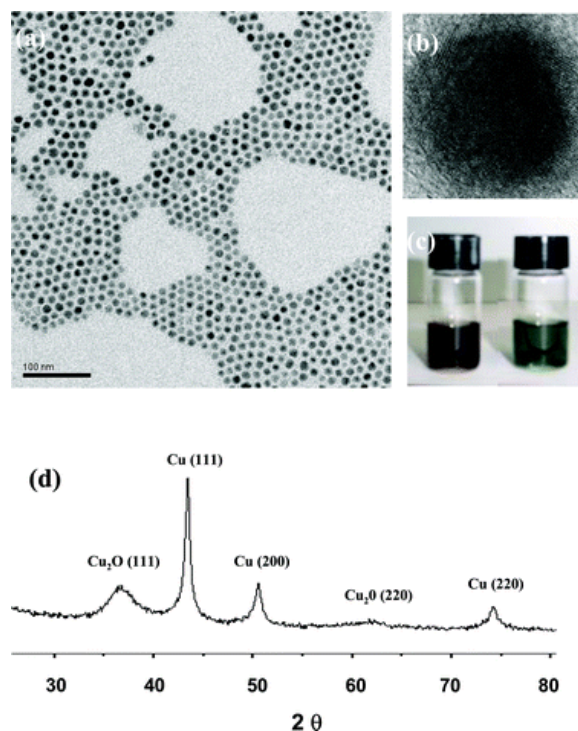


Fig. 8 (a) TEM and (b) HRTEM images of 15 nm Cu₂O coated Cu nanoparticles. (c) Photographs of the colloidal solution containing Cu nanoparticles (left) and Cu₂O coated Cu nanoparticles (right). (d) XRD pattern of Cu₂O coated Cu nanoparticles.

Let's take an example of material chemist to see how they work on Cu-based NPs for C-N coupling reactions. Hyeon and his co-workers reported a synthesis of Cu@Cu₂O nanoparticles through the thermal decomposition of Cu(Ac)₂ in oleylamine.²⁹ After washing there Cu NPs, they will get a core-shell structures because surface Cu(0) will be oxidized by O₂. The structural characterizations are shown in **Fig. 8**. Actually this is a quite common phenomenon because Cu(0) nanoparticles are very active and easy to be oxidized. In most of reports about the application of Cu(0) nanoparticles, they may neglect this problem especially during the catalytic processes. Using these Cu@Cu₂O nanoparticles, they can activate aryl chlorides for Ullmann-type amination coupling reaction. In this paper, they can only active aryl chlorides with electron-withdraw groups. For the less active aryl chlorides such as chlorobenzene and 4-methoxychlorobenzene, these Cu@Cu₂O seems not effective.

Another example for click reaction catalyzed by Cu-based NPs is the Huisgen cycloaddition reaction using magnetically separable Cu nanoparticles as catalyst (**Fig. 9**).³⁰ Compared with soluble Cu complexes, Cu₃N nanoparticles supported on SiO₂ are recyclable catalysts. From the kinetic results, we can see that Cu₃N nanoparticles are comparable with Cu(I) complexes.

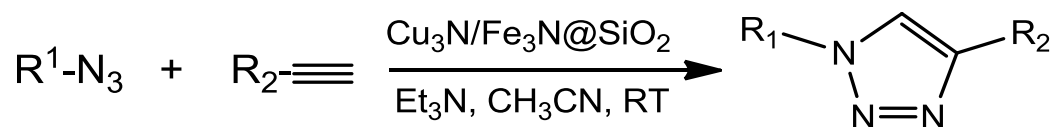


Fig. 9 Huisgen cycloaddition reaction using magnetically separable Cu₃N/Fe₃N@SiO₂ as catalyst.

Based on the above summary of some works on the application of Cu-based NPs for C-N coupling reactions, we can find that there are still lots of unknown questions in this field. For example:

- 1) What's the real active species? For different C-N coupling reaction, the reaction mechanism maybe different. For the N-arylation reaction, since a oxidation addition process is need during the C-N coupling, the transformation of Cu-based NPs are not revealed in previous reaction. The leaching mechanism of Cu-based NPs is proved, so what's the role of the leaching Cu species? For the click reaction (1,3-dipolar Huisgen cycloaddition reaction), surface Cu(I) may be the active sites for this reaction because this reaction is an acid-catalyzed reaction. In most of the previous reports, they just show Cu-based NPs are active for C-N coupling reaction. In some reactions, both Cu⁰, Cu₂O and CuO are active. So, there should be some in-situ generated species that are real active species for these reactions. We need to distinguish which

reaction is homogeneous and which reaction is heterogeneous although they can be catalyzed by Cu-based NPs.

- 2) What are the effects of physiochemical properties of Cu-based NPs on the catalytic performances? For some heterogeneous C-N coupling reaction that occur on the surface of Cu-based NPs, the size and surface structures of Cu-based NPs should have significant effects on the catalytic properties. So far, almost no related works have been reported.

If we can have a further study on these two aspects, I think we can get deeper understanding on the mechanisms about C-N coupling reactions based on Cu or CuOx nanoparticles.

1.3 Stabilizing metal nanoparticles by porous materials

Due to the large numbers of coordination-unsaturated surface atoms, metal clusters tend to aggregate to larger particles under high temperature or during the reaction. Porous materials, especially microporous materials will provide a confined micro-environment, which can protect metal clusters from agglomeration.³¹ The sizes of most pores in zeolites are below 1 nm (as shown in **Fig. 10**), which can serve as the confinement environments to protect metal clusters from sintering and contacting with larger molecules that block active surfaces. Iglesia et al. reported a hydrothermal synthesis of metal clusters (Pt, Pd, Rh and Ru) encapsulated in aluminosilicate zeolites.^{32,33} The encapsulation of metal clusters was achieved through the interaction between metal precursors and incipient aluminosilicate frameworks during hydrothermal process. TEM images of the as-prepared products are presented in **Fig. B11**, from which we can find that clusters around 1.6 nm are confined in the voids. These composites are effective catalysts for the selective hydrogenation-dehydrogenation of reactants smaller than zeolite apertures over larger ones while protecting the active clusters from large organosulfur poisons, which irreversibly bind the active sites.

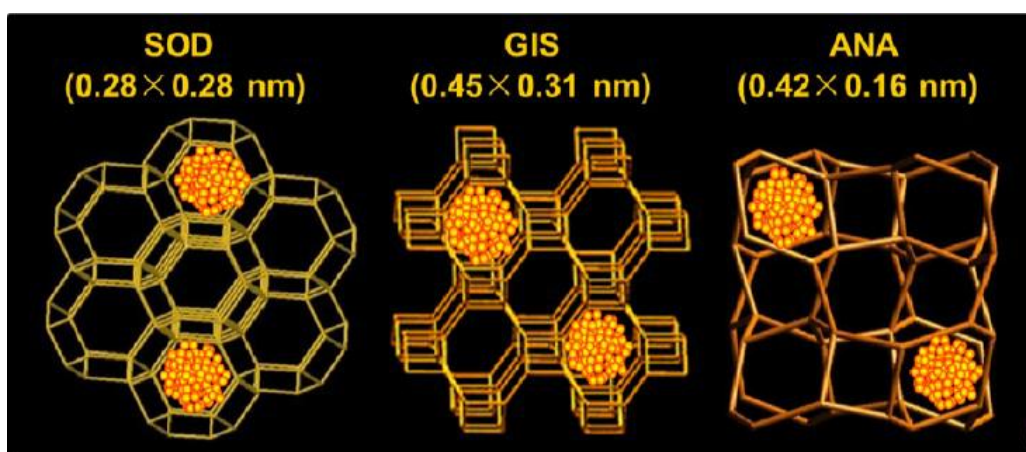


Fig. 10 Pictorial representation of metal clusters encapsulated within zeolites and zeolite aperture sizes.

Combing the decomposition of organic metal compounds and confinement effect of zeolites, Gates et al. can control the size of metal clusters supported on zeolites through the structures of precursor and zeolites. If using $\text{Ir}(\text{CO})_2(\text{acac})$ as the precursor, $\text{Ir}_6(\text{CO})_{16}$ are prepared through a ship-in-bottle synthesis. Then, Ir_6 clusters can be compartmentalized in the supercages of zeolite NaY after decarbonylation (as shown in **Fig. 12**).³⁴ Two bonding positions of the Ir_6 clusters in the supercages were distinguished; 25% of the clusters were present at T5 sites and 75% at T6 sites. These Ir_6 clusters show high activity and selectivity in the hydrogenation of ethane. In another work, mononuclear zeolite-supported Iridium can be obtained using $\text{Ir}(\text{C}_2\text{H}_4)_2(\text{acac})$ as precursor and loaded on zeolite Y through slow evacuation of the solvent.³⁵ Fresh and used catalysts are investigated by HADDF-STEM (**Fig. 13**). The results show that only mononuclear Ir specie can be observed on zeolite Y. Using this mononuclear Ir/zeolite catalyst, the authors proved that atomically dispersed Ir compound can serve as the active site for hydrogenation of cyclohexene at 22-25 °C.

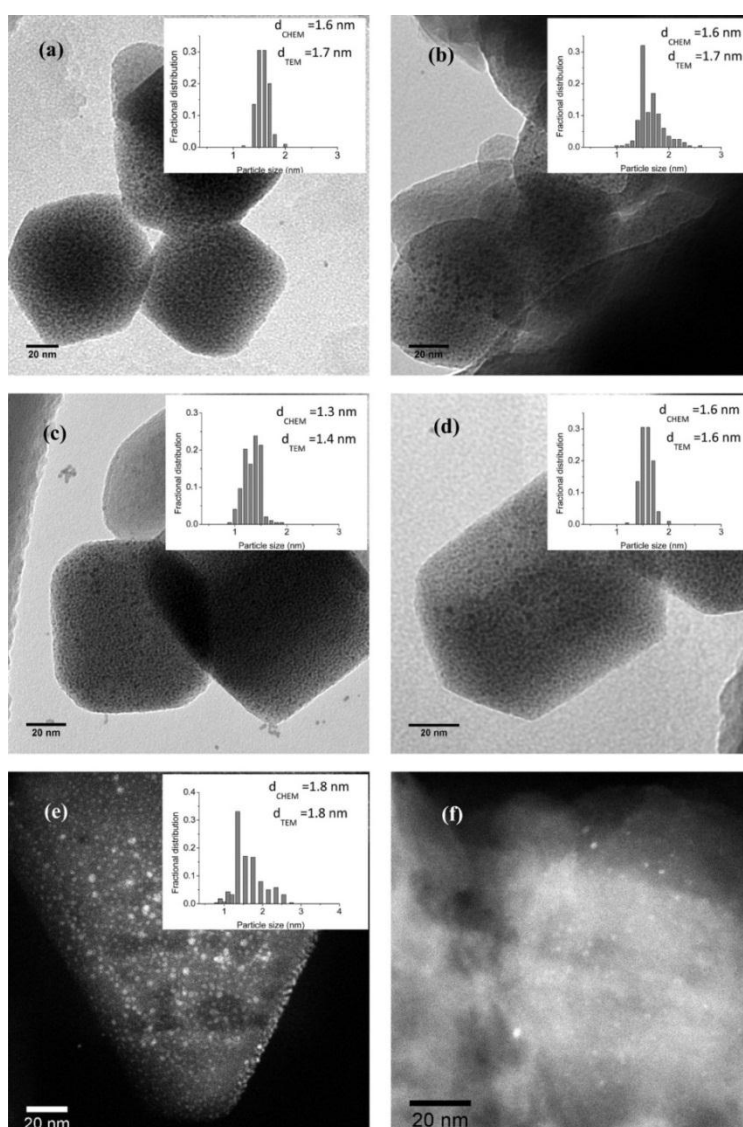


Fig. 11 Metal clusters size distributions and TEM images of (a) Pt/GIS, (b) Pd/GIS, (c) Ru/GIS, (d) Rh/GIS, and HAADF STEM images of (e) Pt/ANA and (f) Pt/SOD samples.

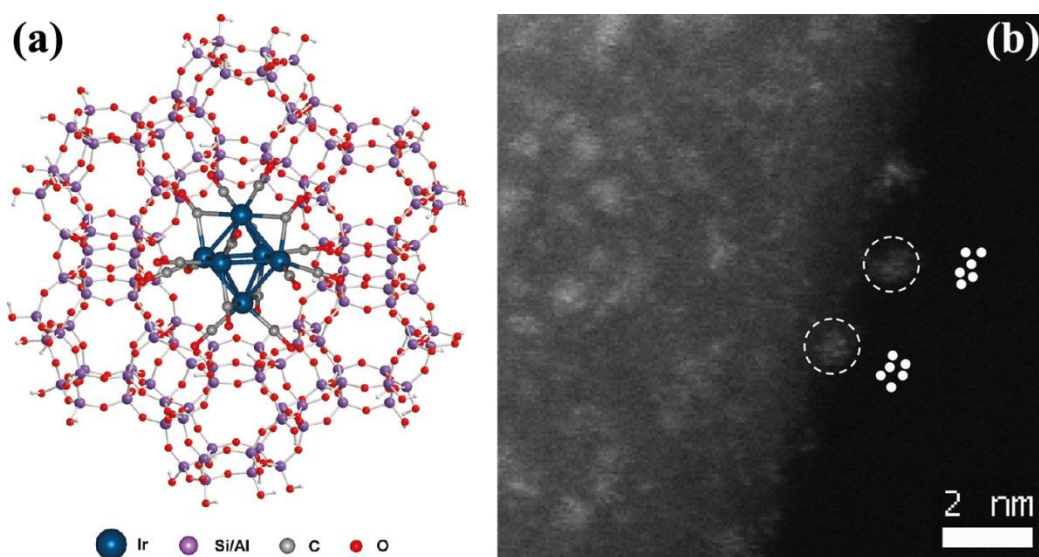


Fig. 12 (a) Schematic representation of $\text{Ir}_6(\text{CO})_{16}$ encapsulated in a supercage of zeolite NaY (a faujasite). (b) Aberration-corrected HAADF-STEM image of zeolite NaY-supported sample containing 10 wt % iridium after decarbonylation of the clusters: image showing Ir_6 clusters with atomic resolution. Superimposed on the image next to two clusters are models of the cluster structures indicating the metal frameworks, which, because of electronbeam damage, are no longer octahedral, as they were in $\text{Ir}_6(\text{CO})_{16}$.

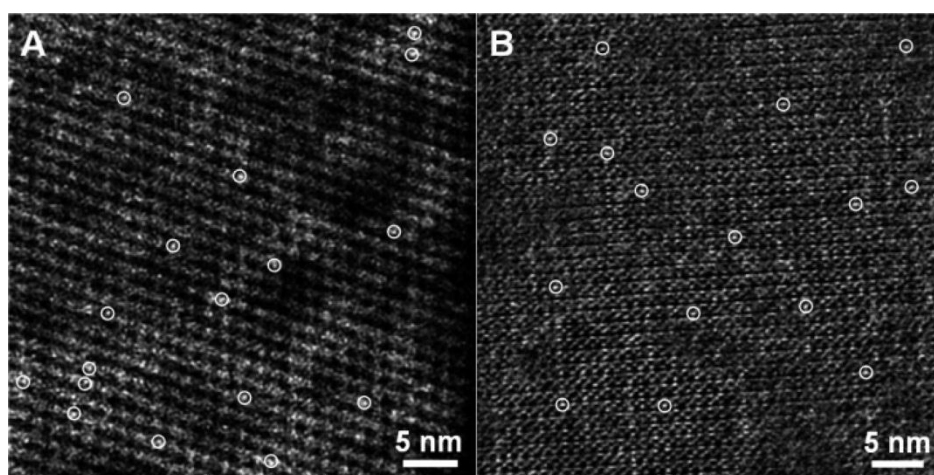


Fig. 13 HAADF-STEM images of (A) initially prepared $[\text{Ir}-(\text{C}_2\text{H}_4)_2]/\text{zeolite Y}$, and (B) the post-catalysis sample. Bright features are the site-isolated, single Ir atoms supported in zeolite Y. A few, representative single Ir atoms are circled to aid their visualization.

Except for zeolites, metal-organic frameworks (MOF) can also be used as the platforms to support metal clusters. The intrinsic porosity and functionality of MOFs make them as promising materials for gas adsorption, separation and catalysis. Incorporating metal clusters into the pore channels of

MOFs can combine their advantages together, resulting in new catalytic materials.^{36,37} A typical synthesis of metal clusters@MOFs is shown in **Fig. 14**. Metal clusters can be produced through the reduction of the precursors and then confined in the metal-organic cages. Their sized can be controlled through tuning the sizes of metal-organic cavities (as shown in **Fig. 15**). In ZIF-90, the aldehyde functionalized imidazolate linkers of ZIF-90 can stabilize drastically smaller Au clusters with a pronounced tendency matching with the cavity size of 1.2-1.3 nm.³⁸ Ultra-small Au₂ and Au₃ clusters can also be prepared with the confinement effect of MOFs.³⁹ Moreover, bimetallic clusters can also prepared using this method.⁴⁰⁻⁴² These bimetallic clusters confined in MOFs show good activities in many reactions, like selective hydrogenation, dehydrogenation of formic acid and selective oxidation. Electronic interactions may exist between the metal clusters and MOFs, leading to synergistic effects on catalytic performances. Besides, through modifying the structures of MOFs, we can build functional cluster-MOFs nanocomposites as functional catalysts.⁴³ In the work of Lin et al., they incorporate Pt clusters into phosphorescent MOFs. The resulting Pt@MOFs assemblies serve as effective photocatalysts for hydrogen evolution by synergistic photo-excitation of frameworks and electron injection into the Pt ultra-small nanoparticles.

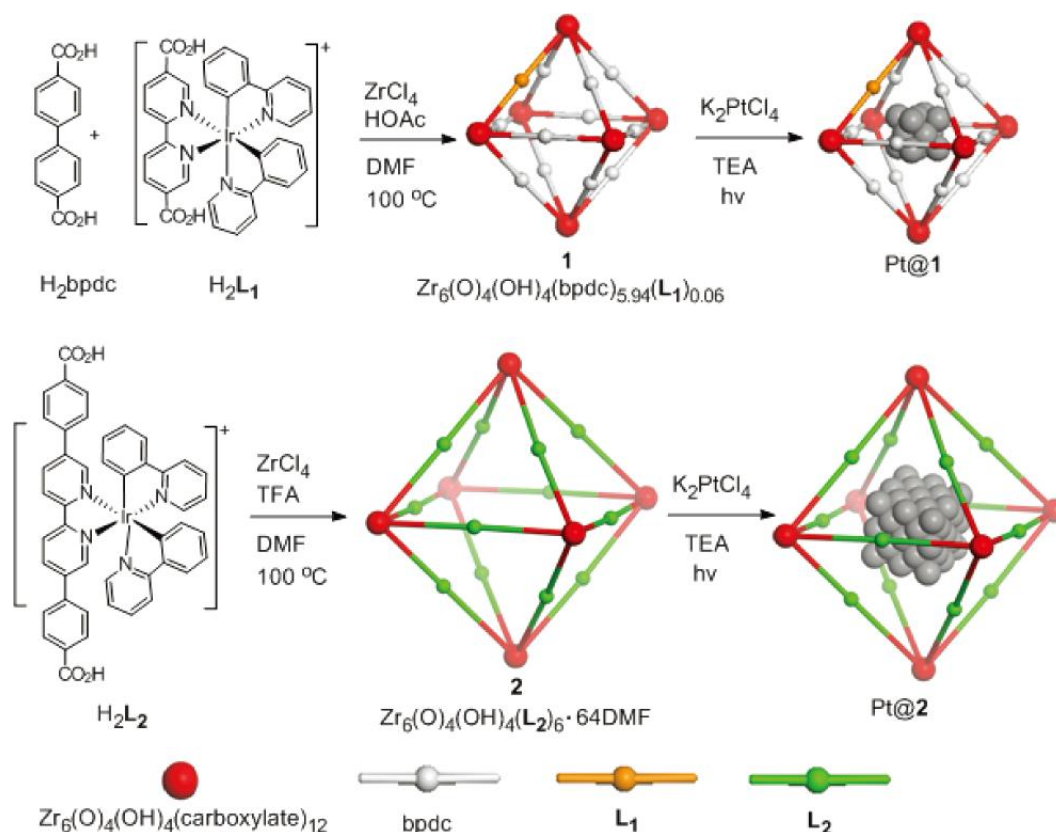


Fig. 14 Synthesis of Phosphorescent Zr-Carboxylate MOFs (1 and 2) of the fcu Topology and Subsequent Loading of Pt NPs inside MOF Cavities via MOF-Mediated Photoreduction of K₂PtCl₄ to Form the Pt@1 and Pt@2 Assemblies.

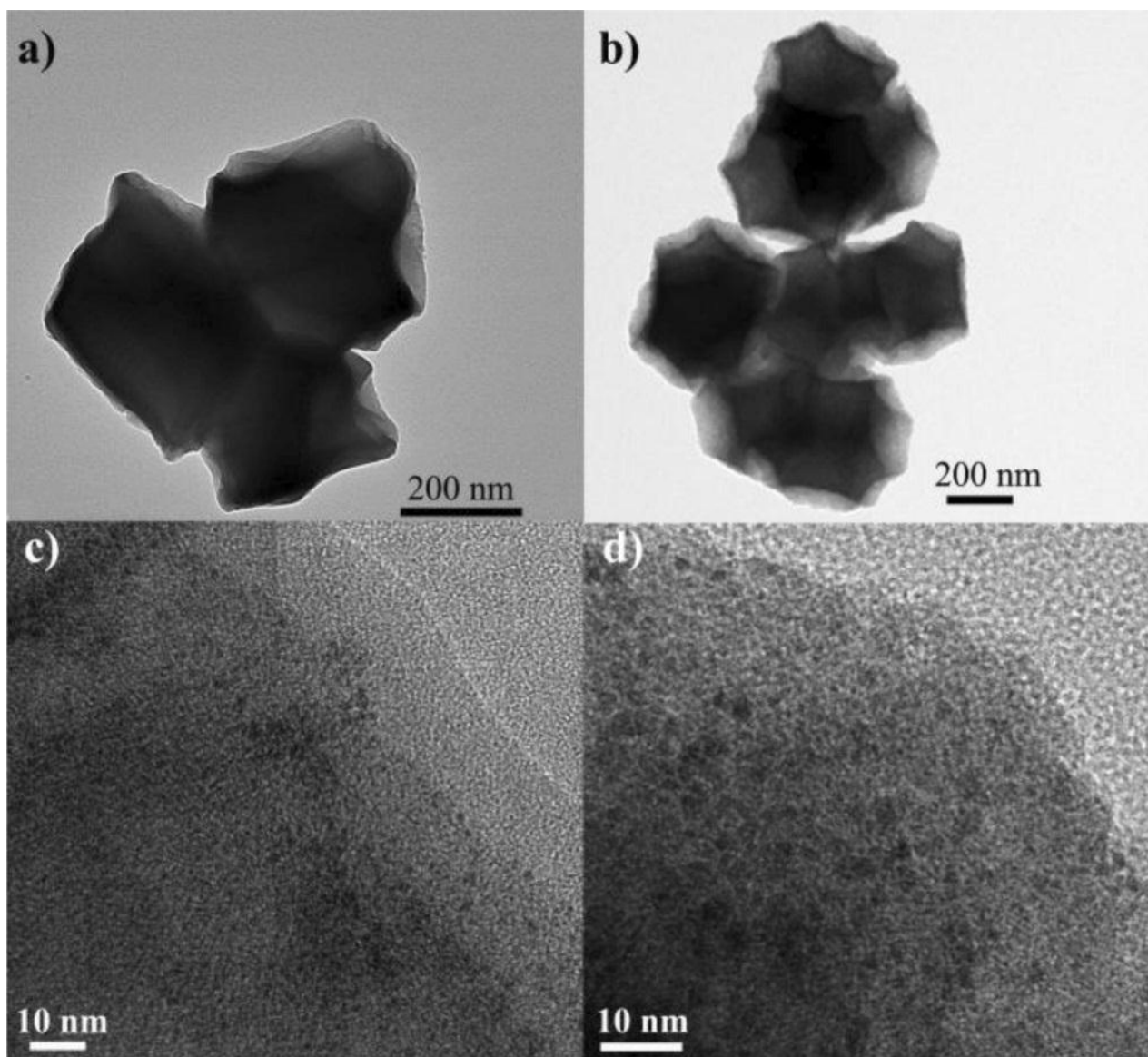


Fig. 15 TEM images of Pt@1 (a and c) and Pt@2 (b and d). The black dots in (c) and (d) are Pt NPs.

2. Cu nanoparticles for C-N coupling reactions

In this part, I will show the application of Cu nanoparticles (NPs) for C-N coupling reactions. Monodispersed Cu nanoparticles are prepared and characterized with XPS and UV-vis. Both fresh Cu NPs and aged Cu NPs are used for C-N coupling reaction. We find that fresh Cu (with more metallic Cu) have better activity than aged Cu NPs (almost totally oxidized). Cu NPs will decompose during C-N coupling reactions and Cu clusters will form in-situ, which should be the active species for C-N coupling reactions.

2.1 Preparation of Cu nanoparticles (NPs)

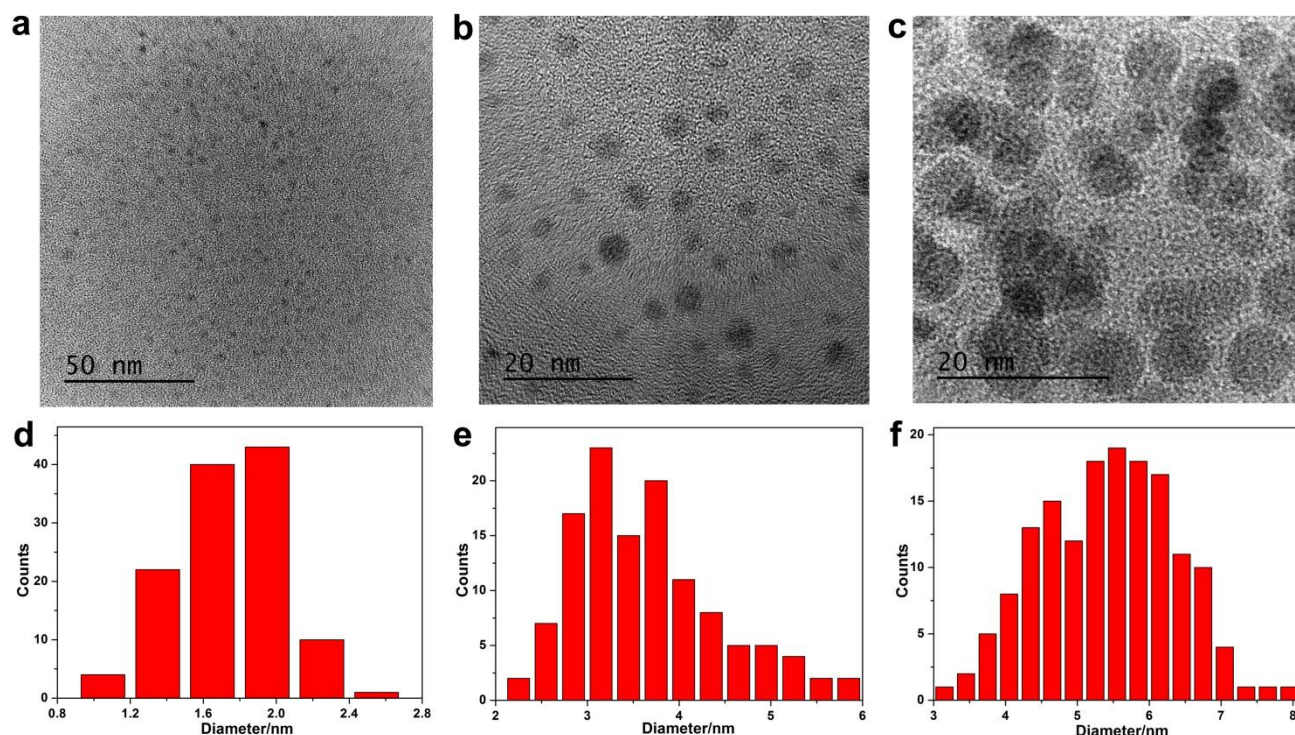


Fig. 16 TEM images of Cu nanoparticles with different sizes. (a, d) 1.5 nm, (b, e) 3.5 nm and (c, f) 5.5 nm.

Cu NPs are synthesized by a NaBH_4 reduction method. PVP (55,000) is used as the capping agent and the size of Cu NPs can be controlled by the amount of PVP. For the synthesis of Cu NPs (~1.5 nm), the procedure is described as following. 30 mg $\text{Cu}(\text{Ac})_2$ is dissolved in 20 mL ethylene glycol (EG) at room temperature. Then 0.5 mL 1 mol/L NaOH EG solution is added to the $\text{Cu}(\text{Ac})_2$ EG solution. Color change from green to blue can be observed. After stirring for 10 min, 50 mg NaBH_4 is added to the above blue solution and keep stirring for 1 h. Afterwards, Cu^{2+} is totally reduced by NaBH_4 and red suspension of Cu NPs can be obtained. After adding 40 mL acetone (with 15 mg NaBH_4), Cu NPs can be isolated by centrifugation at 15,000 rpm for 30 min. Then those Cu NPs are dispersed in DMF for C-N coupling reactions. In order to prepare Cu NPs of 3.5 nm and 5.5 nm, 30

mg PVP and 100 mg PVP are added, respectively. The other operation details are similar with that for the synthesis of Cu NPs (~1.5 nm).

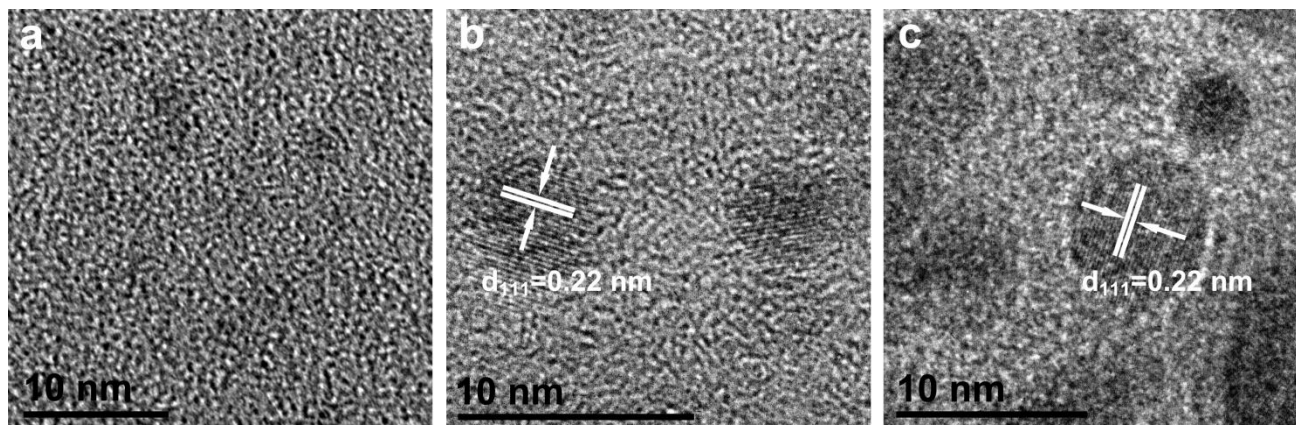


Fig. 17 HRTEM images of Cu NPs. (a) 1.5 nm, (b) 3.5 nm and (c) 5.5 nm.

TEM images of three Cu NPs samples are shown in Fig. 16. Size distributions of three samples are also displayed. The average sizes are 1.5 nm, 3.5 nm and 5.5 nm. HRTEM images show these particles are metallic copper, with crystal lattice fringe corresponding to {111} planes of Cu.

2.2 C-N coupling reaction activities

For C-N coupling reactions, both newly prepared Cu NPs and Cu NPs that are kept in the lab for one day after synthesis. The reaction conditions and the amount of Cu NPs used is given in the schemes.

From **Fig. 18a**, we can see that newly prepared Cu NPs are more active than Cu NPs that are kept for one day. For newly Cu NPs, they have more metallic Cu compared with those are kept for one day. More interestingly, for fresh Cu NPs, small Cu NPs have better activities than larger Cu NPs. However, for Cu NPs have been kept for one day, activities of small Cu NPs decrease dramatically. Cu NPs of 5.5 nm show similar activity for both samples, suggesting that they are more stable than the small Cu NPs. During one day in the lab, Cu NPs will be oxidized by air, leading to the formation of surface oxidized Cu NPs (Cu@CuOx). Small Cu NPs are much easier to be oxidized by air, so an apparent decrease can be observed. For large Cu NPs, they are more stable, so the activities for both 5.5 nm Cu NPs are closed. In this C-N coupling reactions, we need metallic Cu species. So, newly prepared Cu NPs are more active than Cu NPs-one day.

A short induction time (5~6 min) can also be observed in **Fig. 18b**. This induction time is much shorter than Cu salts. This induction time can be ascribed to the leaching of Cu NPs to Cu clusters and the reduction of Cu oxides to metallic Cu.

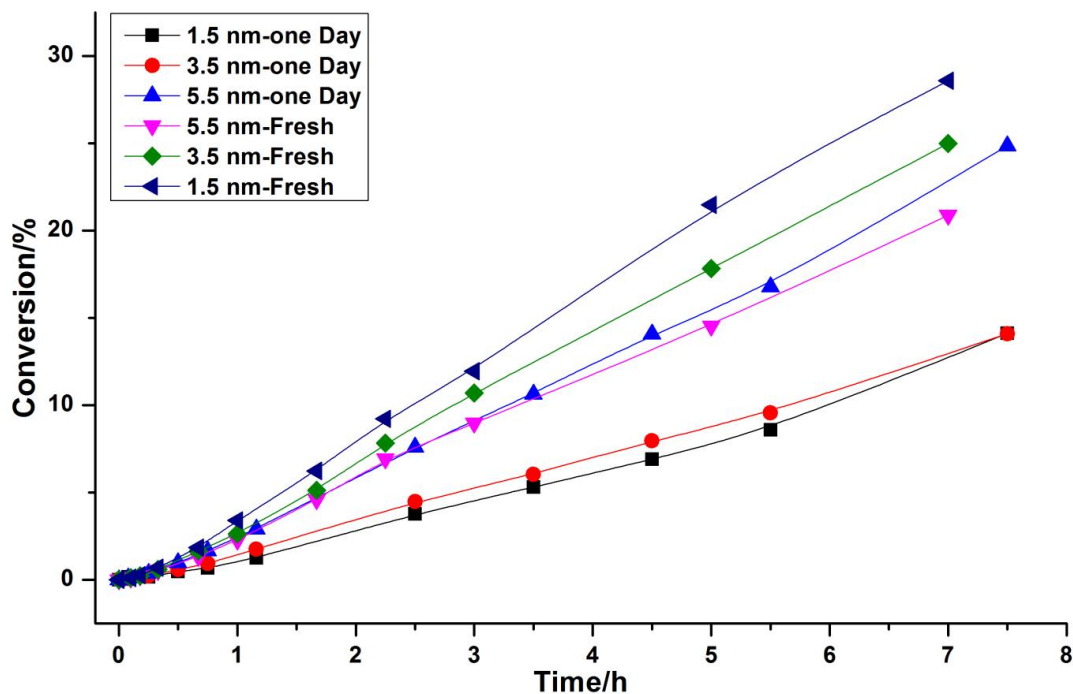
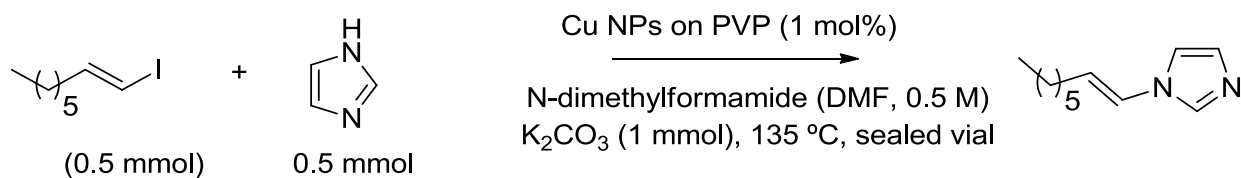


Fig. 18a Activity of Cu NPs in C-N coupling reactions.

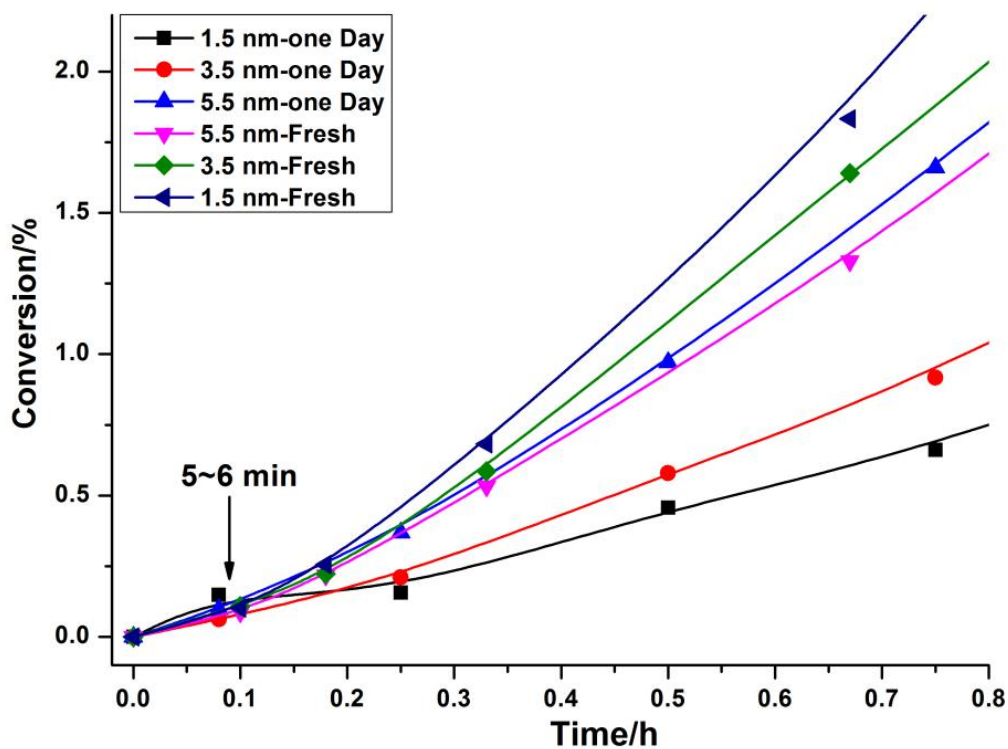


Fig. 18b Activity of Cu NPs in the starting stage.

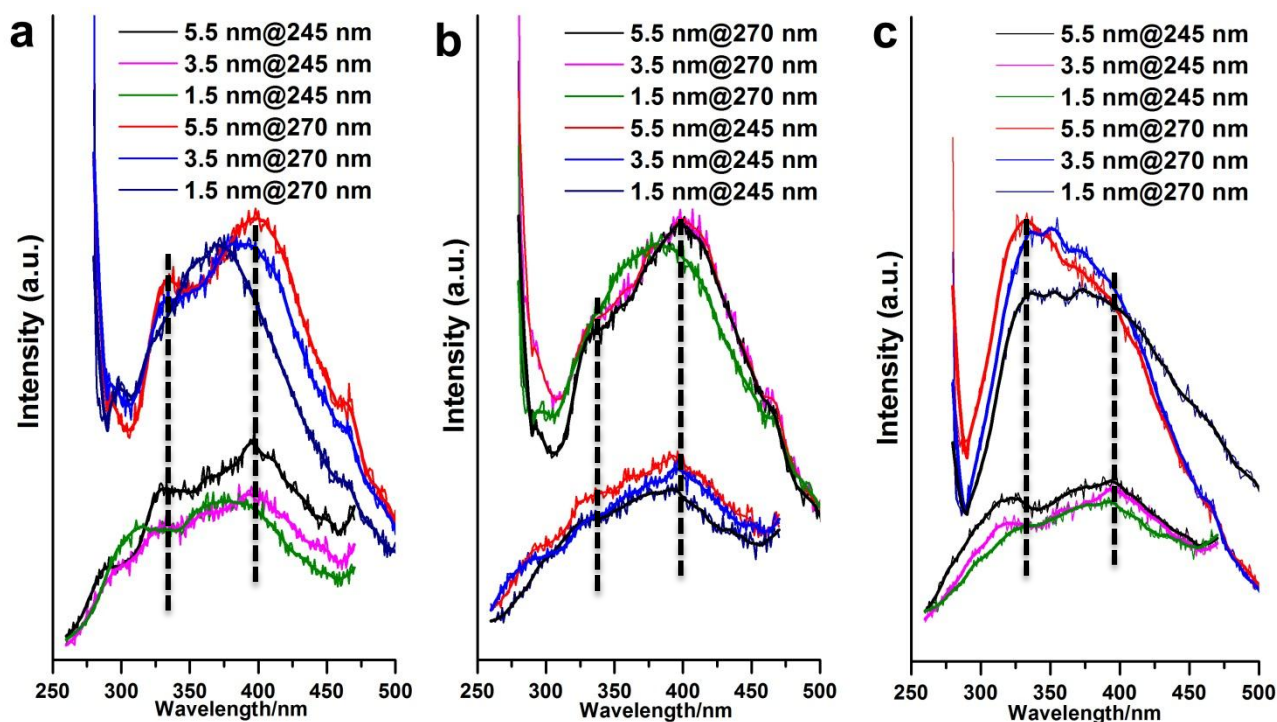


Fig. 19 Fluorescence spectra of the reaction mixture during C-N coupling reactions by fresh Cu NPs at different time. (a) 5 min, (b) 30 min and (c) 2 h.

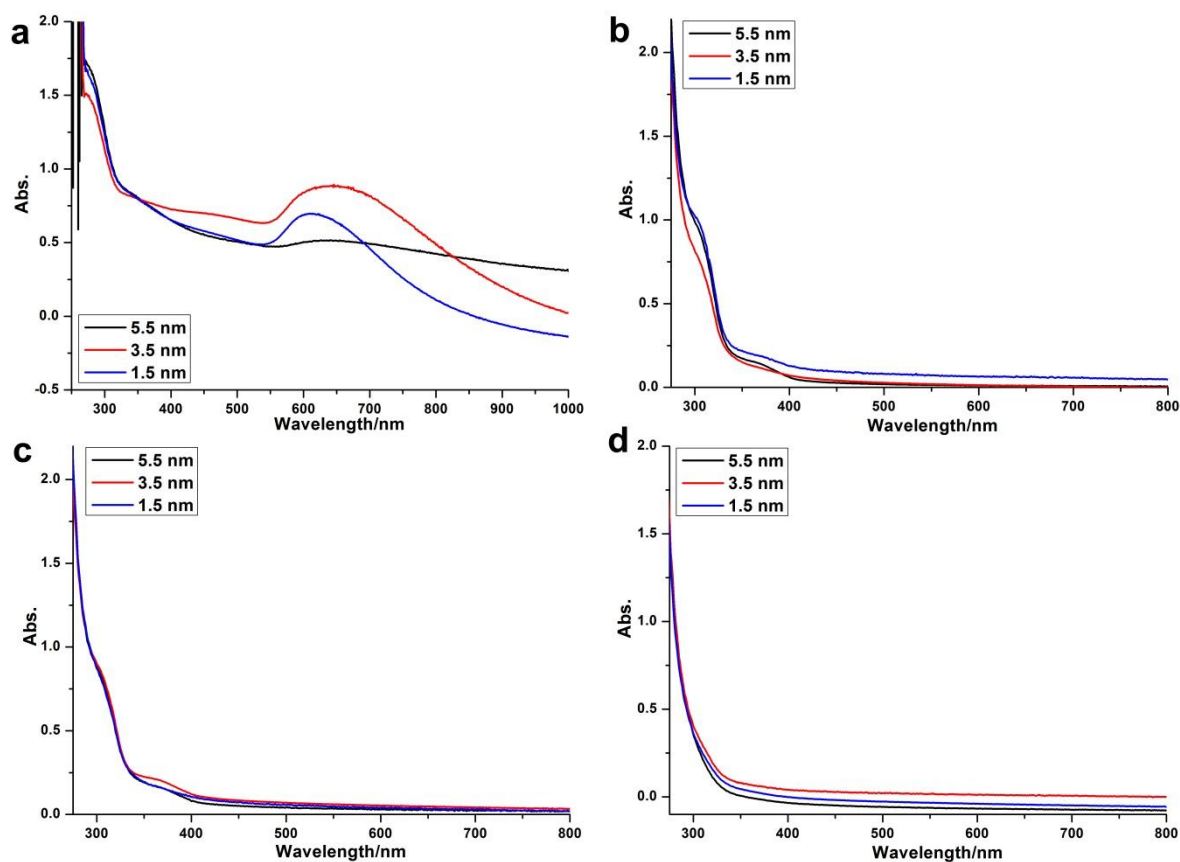


Fig. 20 UV-vis spectra of the reaction mixture during C-N coupling reactions by fresh Cu NPs at different time. (a) Fresh Cu NPs, (b) 5 min, (c) 30 min and (d) 2 h.

From fluorescence spectra in **Fig. 19**, clusters are formed at the starting stage. Peaks located around 325 nm and 400 nm can be ascribed to Cu_{2-3} and Cu_5 clusters. These Cu clusters should come from the leaching of Cu NPs. From the UV-vis spectra (**Fig. 20**), we can also see the evolution of Cu NPs during the reactions. For fresh Cu NPs, we can see one peak at around 300 nm and 350 nm, which are corresponding to CuOx. For the peaks at 550 nm to 800 nm, they are d-d transition of CuOx. The plasmon peaks of metallic Cu are not visible in UV-vis spectroscopy because the surface of Cu NPs is partially oxidized. After reaction for 5 min and 30 min, the peaks corresponding to CuOx can still be seen while the peaks corresponding to d-d transition disappear. After reaction for 5 h, the peaks corresponding to CuOx also disappear.

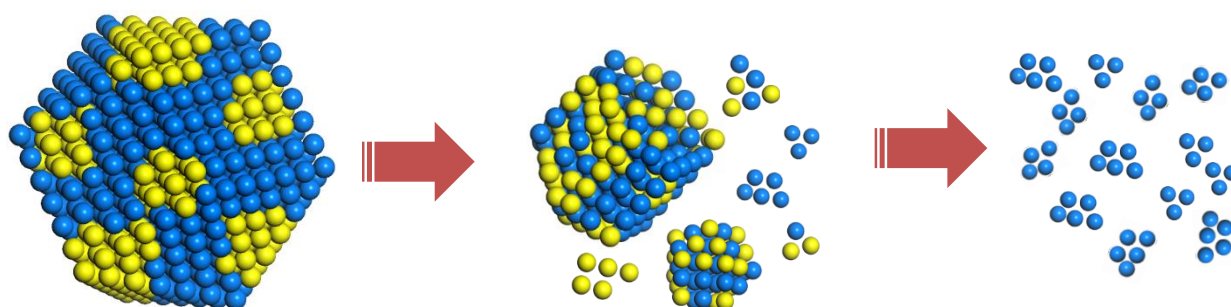
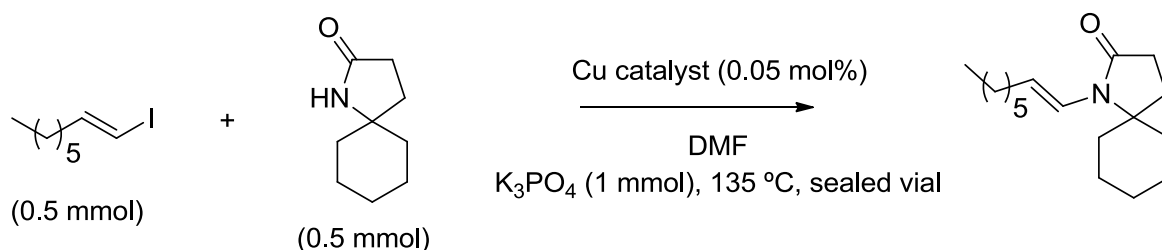


Fig. 21 Schematic illustration of evolution process of Cu NPs (yellow balls stand for CuOx while blue balls stand for metallic Cu).

Based on the above analysis, we can discuss the evolution process of Cu NPs during the C-N coupling reactions. A schematic illustration is presented in **Fig. 21**. At the starting stage (first 30 min), Cu NPs will be decomposed to fragments with the help of substrate molecules and form some clusters. These clusters maybe partially oxidized Cu clusters. These Cu_xO_y clusters will gradually be reduced during C-N coupling reactions and form active metallic Cu clusters for C-N coupling reactions.



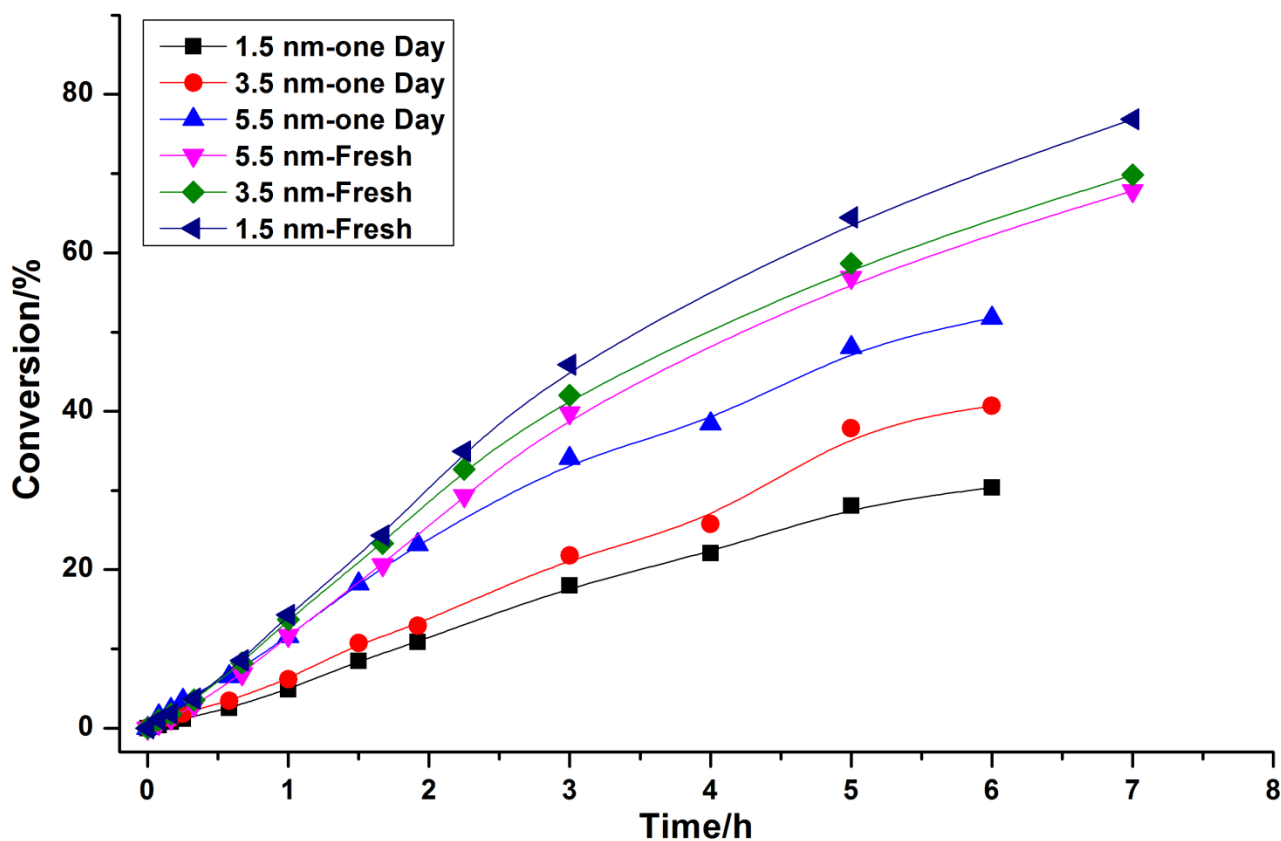


Fig. 22 Activity of Cu NPs in C-N coupling reactions using amide as substrate molecule.

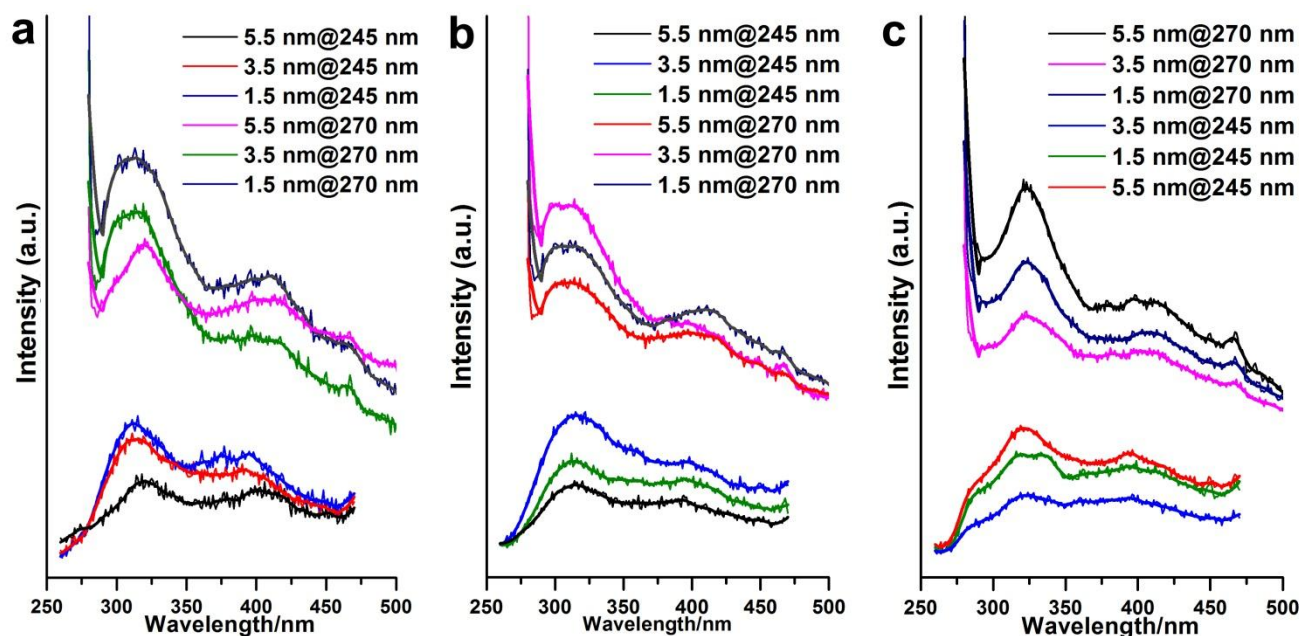


Fig. 23 Fluorescence spectra of the reaction mixture during C-N coupling reactions with amide by fresh Cu NPs at different time. (a) Fresh Cu NPs, (b) 5min, (c) 30 min and (d) 2 h.

Similar results have also been obtained in another C-N coupling reaction (Fig. 22). When amide is used for this reaction, the C-N coupling reaction rate is improved significantly. No obvious induction time can be seen for this reaction. Fluorescence and UV-vis spectra also confirm that metallic Cu

clusters (2~5 atoms) are formed very fast at the starting stage. This different should originate from the different reactivity of substrate molecules. Similar evolution from Cu NPs to Cu clusters can also be seen from these data.

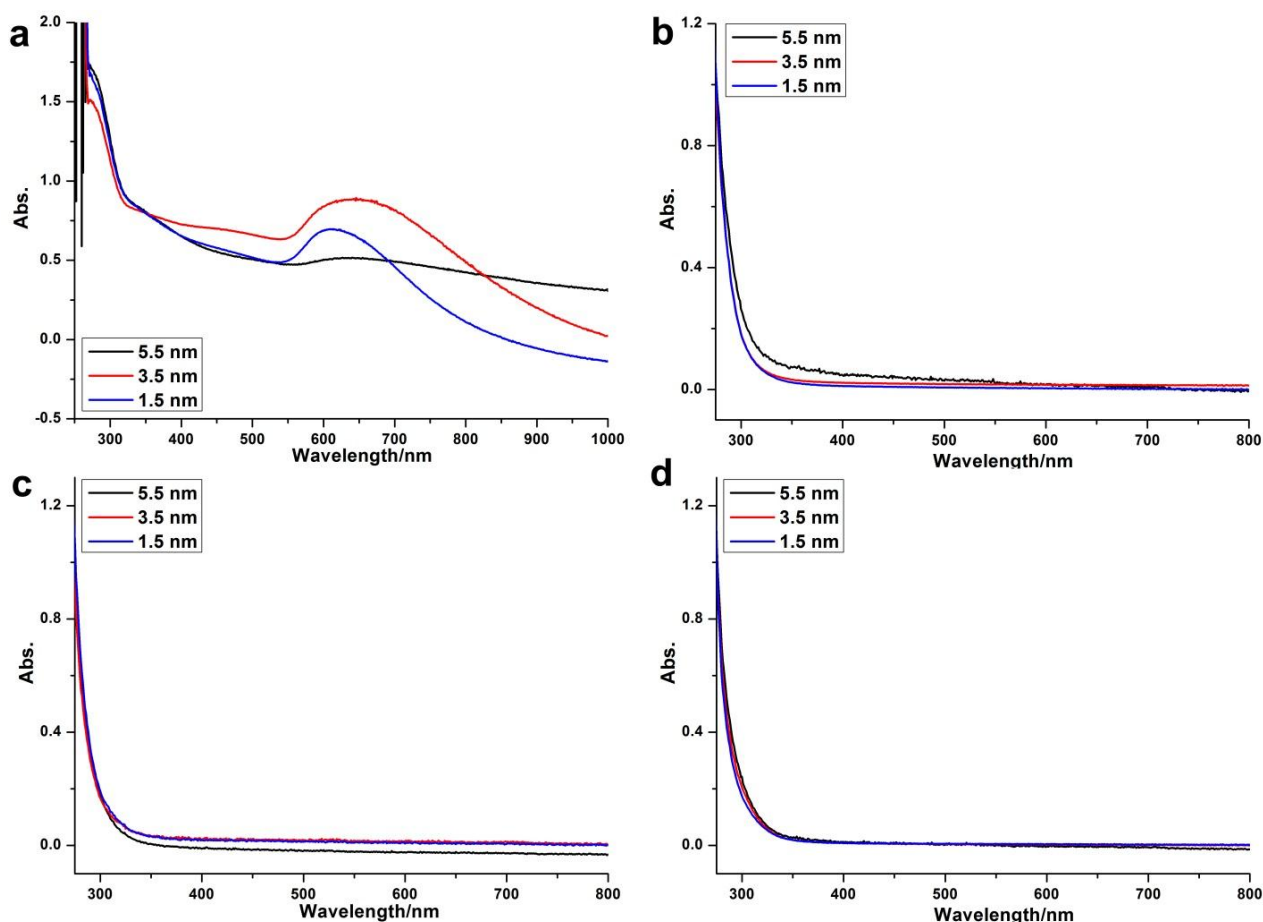


Fig. 24 UV-vis spectra of the reaction mixture during C-N coupling reactions with amide by fresh Cu NPs at different time. (a) Fresh Cu NPs, (b) 5 min, (c) 30 min and (d) 2 h.

2.3 Conclusions

In this part, we use monodispersed Cu NPs for C-N coupling reactions. The results show that reduced Cu NPs can be active catalysts for C-N coupling reactions. These partially oxidized Cu NPs will be reduced and leached into Cu clusters during C-N coupling reactions. When Cu NPs are totally oxidized by air, the activities in C-N coupling reactions will decrease. According to the fluorescence spectra, Cu clusters with 2~5 atoms maybe the active species for C-N coupling reactions.

3 Ultra-small Pt nanoparticles confined in MCM-22

In this part, I will show some recent works on synthesizing ultra-small Pt nanoparticles confined in MCM-22. We want to use layered zeolite (MCM-22) to stabilizing Pt nanoparticles for dehydrogenation of propane to propylene reaction because the aggregation of Pt nanoparticle is the neckbottle for this reaction.

3.1 Experimental details of synthesis

Synthesis of ultra-small Pt nanoparticles

Pt nanoparticles are prepared by a DMF-reduction method. 10 mg $\text{Pt}(\text{acac})_2$ are dissolved in 40 mL DMF. Then the solution is heated at 140 °C for 16 h.

Synthesis of ITQ-1 and Swelled ITQ-1

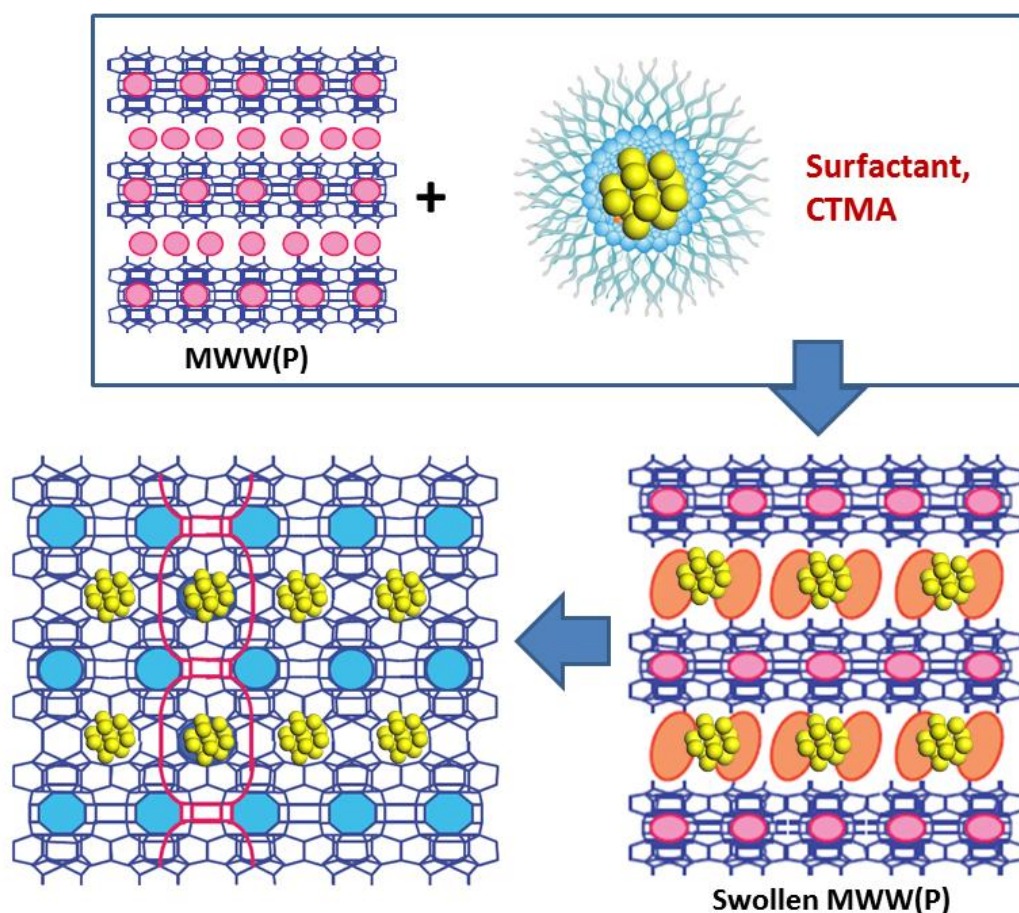
The zeolite ITQ-1 (IZA code MWW) is the pure silica analog of MCM-22. It can be synthesized using trimethyladamantammonium (TMAda^+) as structure directing agent in absence of alkali cations, but serious reproducibility problems appeared. If hexamethyleneimine (HMI) is added as second SDA, the reproducibility of the synthesis, as well as the quality of the materials obtained, are greatly improved. As TMAda^+ is too large to fit into the sinusoidal 10MR channel, this has to be stabilized by some other molecules. In absence of HMI, these probably come from either the partial degradation of TMAda^+ or from organics adsorbed on the PTFE liners in previous synthesis. The use of TMAda^+ , HMI and sodium cations allows a fast and highly reproducible synthesis of pure silica ITQ-1.

An example of the procedure for the synthesis of ITQ-1 using TMAda^+ , HMI and Na^+ cations is as follows: 0.95 g of NaCl are dissolved in 50.70 g of a solution 0.42M of N,N,N trimethyl-1-adamantanammonium hydroxide, previously diluted with 21.33 g of water. Then, 2.62 g of hexamethyleneimine are added to this solution, followed by 4.88 g of silica (Aerosil 200, Degussa) under continuous stirring. This reaction mixture is heated in a PTFE lined stainless steel autoclave at 150 °C rotated at 60 rpm for 5 days. After filtering, the white solid obtained is washed until pH was less than 9.

In order to prepare the swelled purely siliceous ITQ-1 with ultra-small Pt nanoparticles, 10 g of the lamellar precursor were dispersed in 40 g of H_2O milliQ, and 200 g of a cetyltrimethylammonium hydroxide solution (25%wt, 50% exchanged Br^-/OH^-) and 60 g of a solution of tetrapropylammonium hydroxide (40%wt, 30% exchanged Br^-/OH^-) were added together with the Pt DMF solution, being the final $\text{pH} \geq 12.5$. The resultant mixture was heated at 325 K, stirring vigorously, for 16 hours in order to facilitate the swelling of the layers of the precursor

material. At this point, the solid was recovered by centrifugation and washed with distilled water, being dried at 333 K for 12 hours.

3.2 Results and discuss



Scheme 2 Schematic illustration of preparation of Pt@MCM-22.

MCM-22 has layered structures and has “cups” around 0.7 nm.⁴⁴ Metal nanoparticles can be captured by these cups and stabilized. And the layered structures can also provide diffusion pathway for dehydrogenation of propane.

The preparation method for Pt@MCM-22 is presented in Scheme 2. In order to incorporate ultra-small Pt NPs into the layers of MCM-22, we need prepare MWW precursor (MWW(P)). Then, The incorporation of Pt NPs can be processed during the swelling process of MWW(P). After swelling, Pt NPs will be encapsulated by MWW layers as well as the surfactants. Then, organic surfactants can be removed by calcination in air, leading to formation of sandwich-like structures, Pt@MCM-22.

TEM image of Pt NPs is shown in Fig. 25. Monodispersed Pt NPs can be seen with average size of ~1 nm. These Pt nanoparticles should be capped by DMF. STEM images of Pt@MCM-22 can be seen in **Fig. 26**. When the heating rate is 2 °C/min, no large Pt NPs can be found on MCM-22 (as shown in **Fig. 26a**). In the images with higher magnification, we can see ultra-small Pt NPs are

dispersed on MCM-22. The average size is ~ 1 nm, suggesting that no obvious aggregation can be found after calcination treatment.

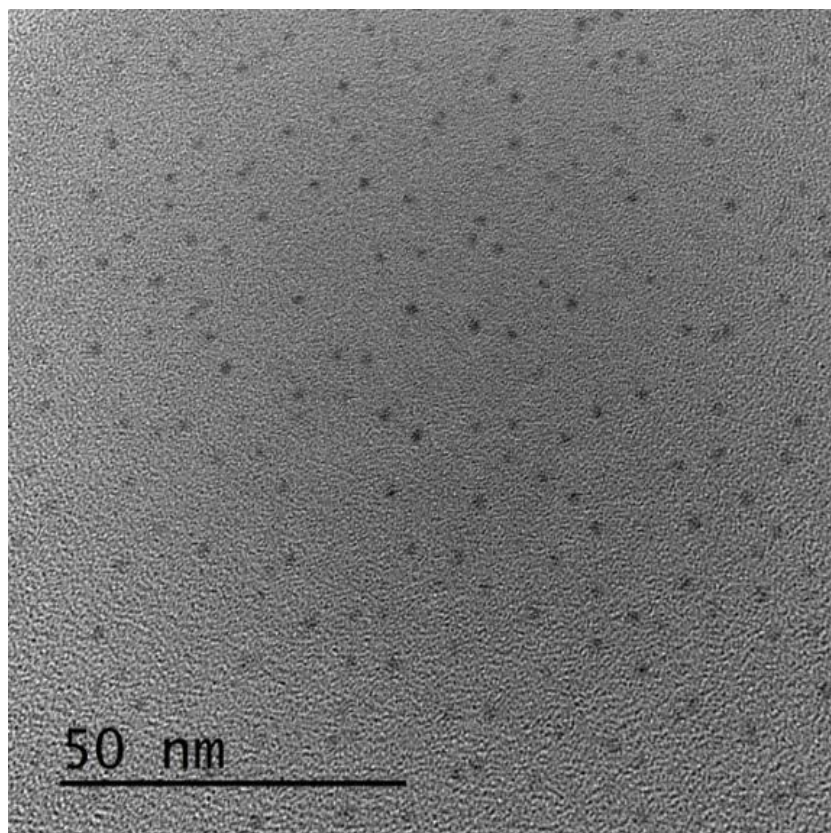


Fig. 25 TEM images of ultra-small Pt nanoparticles.

When the speed of heating during calcination increases to 3 $^{\circ}\text{C}/\text{min}$, the size distributions of Pt NPs will change. In **Fig. 27a**, we can see several large Pt NPs in a large area. These Pt NPs are $5\sim 10$ nm, which should come from the aggregation of Pt NPs outside of MWW layers during the calcination treatment at 540 $^{\circ}\text{C}$. In **Fig. 27b**, we can see ultrafine Pt nanoparticles are dispersed on MCM-22 with average size of ~ 1.5 nm. The average size of Pt NPs grows a little large because of the fast heating during calcination process.

We also test the stability of these Pt nanoparticles under harsh conditions: reduction-oxidation cycles at 650 $^{\circ}\text{C}$. As shown in **Fig. 28**, size of Pt NPs can be preserved after 2 cycles at 650 $^{\circ}\text{C}$. The average size of Pt NPs is between $1\sim 2$ nm, indicating that sandwich-like structures can improve the stability of Pt NPs. However, after 4 cycles of reduction-oxidation treatment, aggregation of Pt nanoparticles can be observed. Small Pt NPs will move together and show local enrichment in STEM images. The size of “cups” of MWW layers are about 0.7 nm but our Pt NPs are larger than the “cups”, which means these MWW layers will be expanded by Pt NPs. As a result, the three dimensional structures of MCM-22 are not complete, which means Pt NPs are not totally captured by MWW layers. At harsh conditions of reduction-oxidation treatments, Pt NPs may aggregate driven

by the high-temperature treatments, because Pt nanoparticles can diffuse and move during the high-temperature treatments.⁴⁵

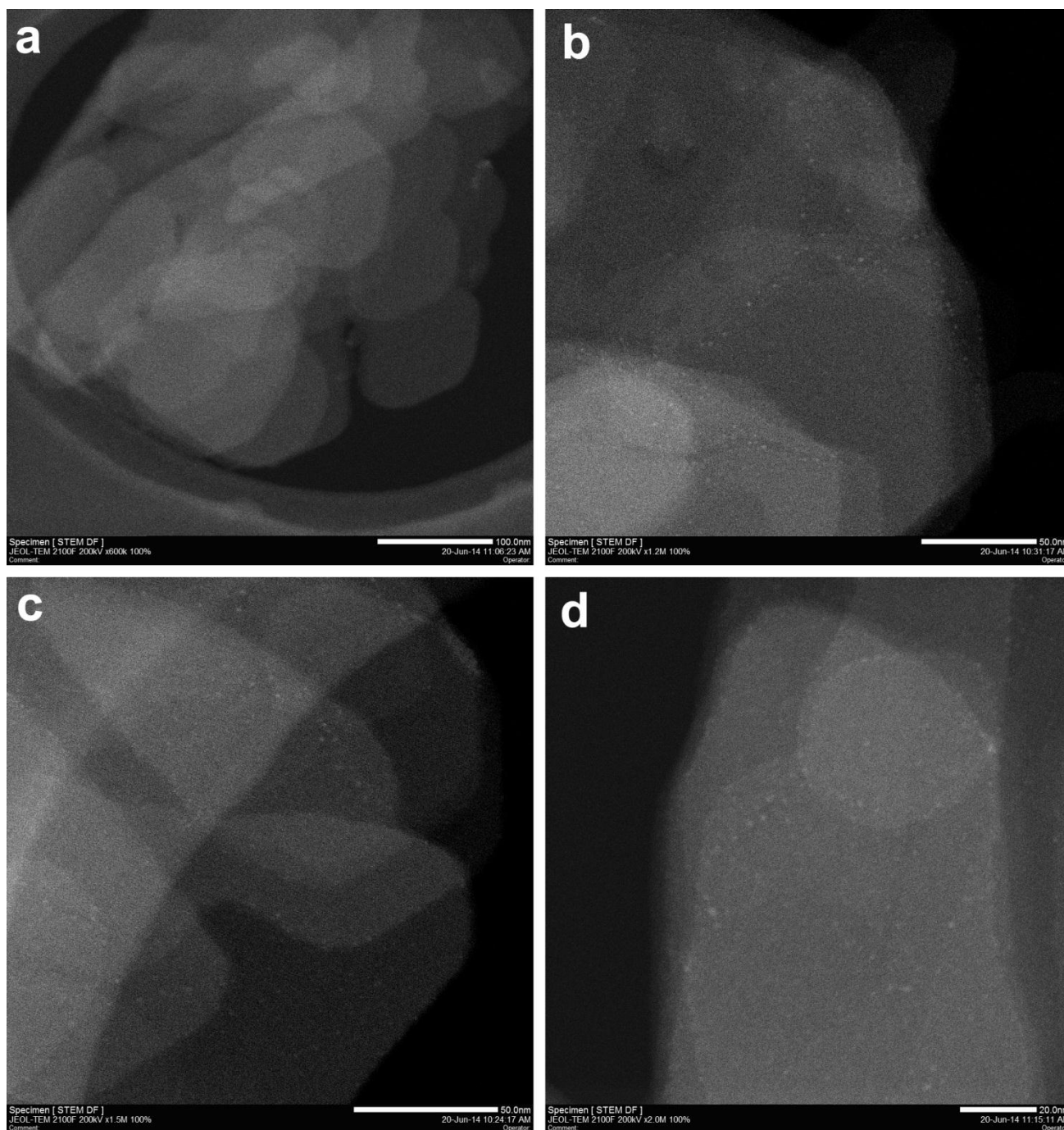


Fig. 26 STEM images of Pt@MCM-22 with a speed of 2 °C/min during calcination.

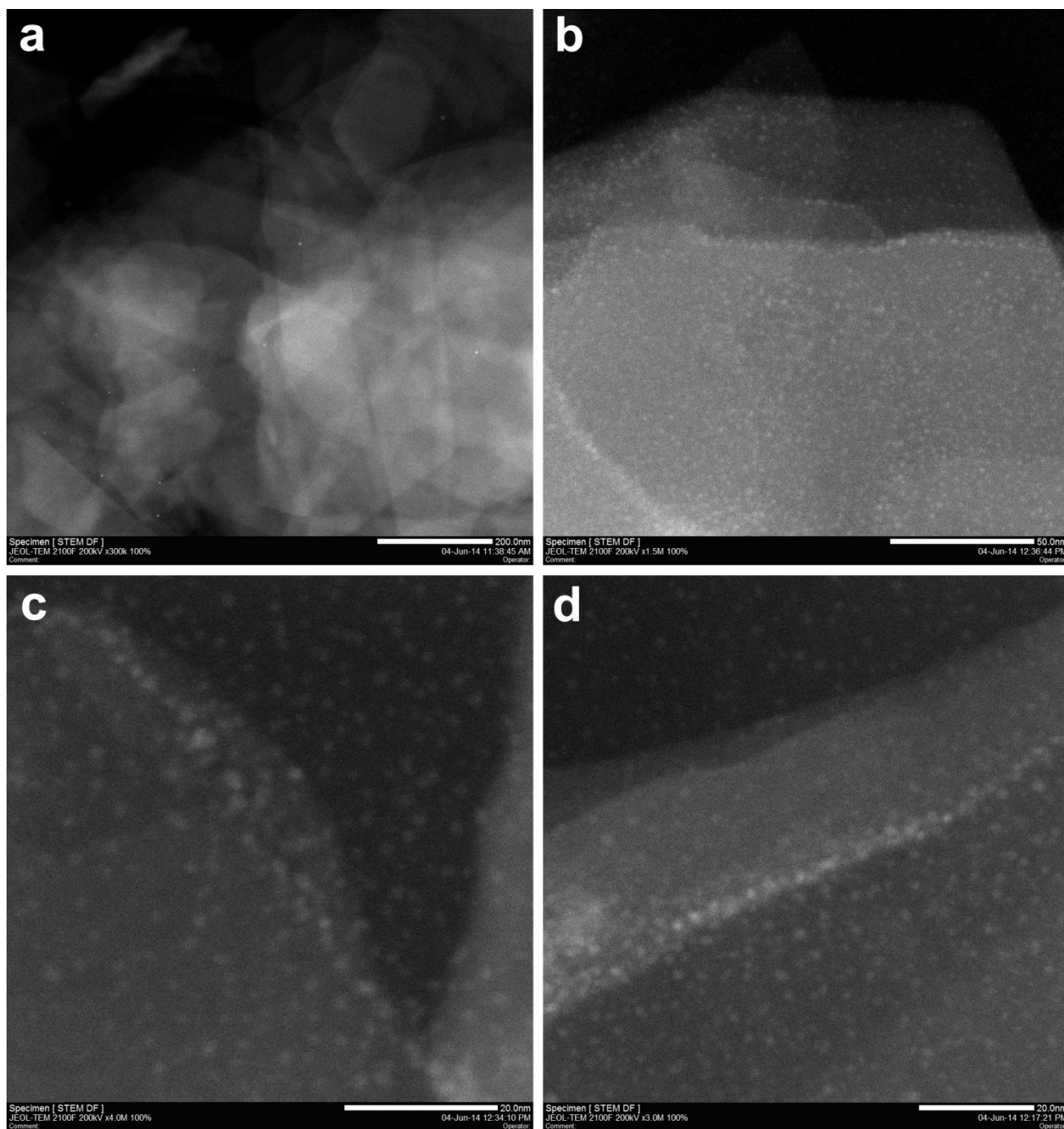


Fig. 27 STEM images of Pt@MCM-22 with a speed of 3 °C/min during calcination process'

3.3 Conclusions

Through this method, ultra-small Pt NPs (~1 nm) can be incorporated into the frameworks of MCM-22. MCM-22 can stabilize these ultra-small Pt NPs, even at 650 °C in H₂ and O₂ atmosphere. This Pt@MCM-22 can be used for dehydrogenation of propane to get propylene.⁴⁶ More works are undergoing in this project. Characterizations and catalytic properties will be tested in the near future.

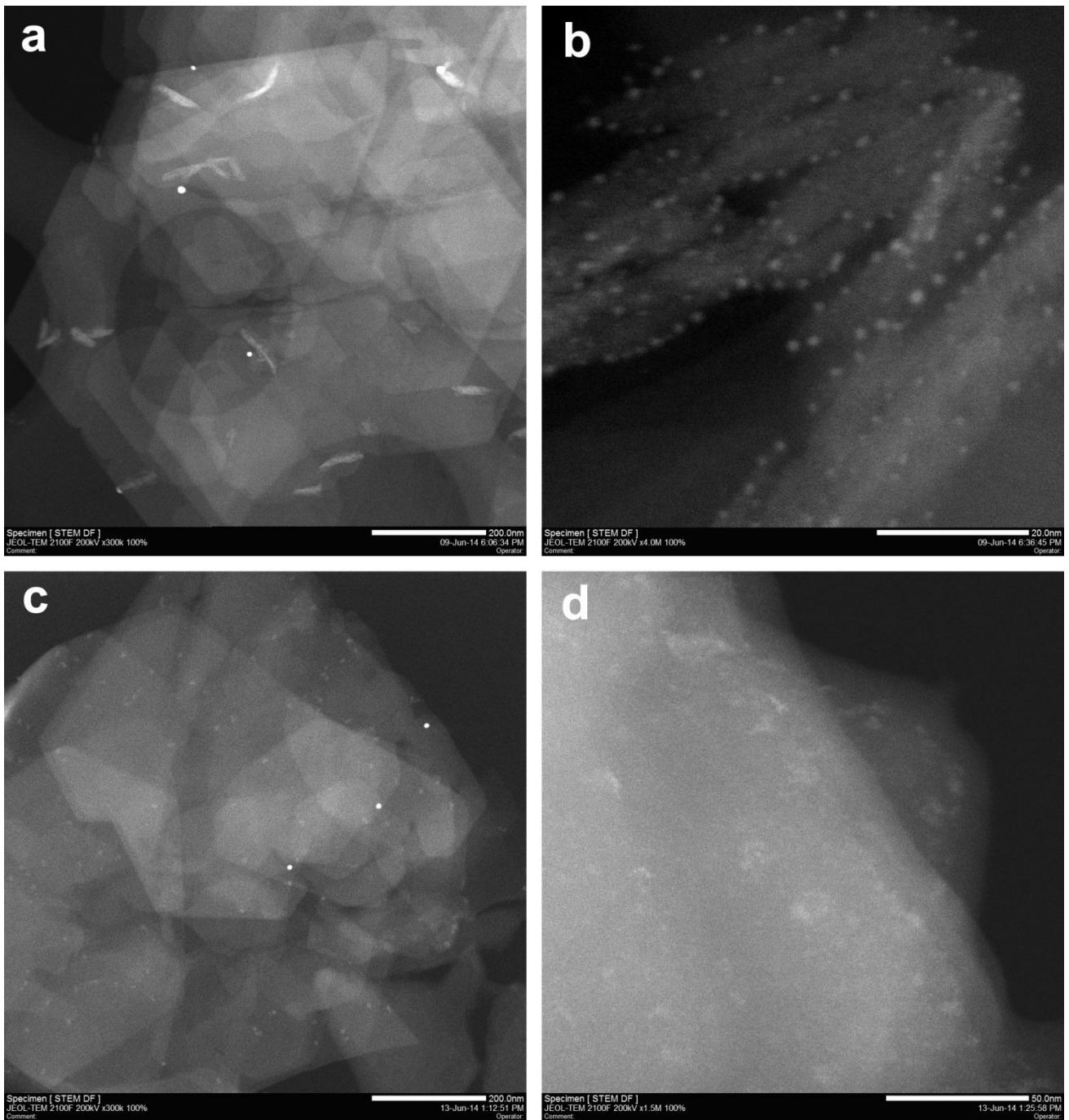


Fig. 28 STEM images of Pt@MCM-22 after reduction-oxidation treatment at 650 °C. (a-b) 2 cycles, (c-d) 4 cycles.

4. Perspectives

Catalysis based on metal clusters and ultra-small metal nanoparticles is an emerging field in catalysis. Exited progresses have been achieved in this field both in experimental and theoretical aspects. However, there are still some crucial questions waiting for being answered:

- 1) **Developing facile and efficient methodologies for the synthesis and stabilization of metal clusters and ultra-small nanoparticles with excellent catalytic performances.** So far, there isn't a facile and controllable method to obtain active metal clusters with large production and controllable atomicity. Furthermore, the stabilization of metal clusters is also important. Developing some method that can not only stabilize the metal clusters, but also do not deactivate the active sites is a big challenge.
- 2) **The mechanisms about the dynamic electronic and geometric transformation processes.** The flexible electronic and geometric structures are the most important key factors accounting for the unique catalytic properties of metal clusters. However, we almost know nothing about this process except for some theoretical calculations. Using ultrafast spectroscopy we may know more about the evolution mechanisms of clusters.
- 3) **The catalytic mechanisms of metal clusters and ultra-small nanoparticles on the supports and in solution.** To achieve these goals, firstly we need to build more advanced instruments to "watch" and "detect" metal clusters. These instruments or characterizations should better be *in-situ* performed. Secondly, theoretical studies should provide more information about clusters and related mechanisms to complement the experimental results.

Based on the fundamental research, we should try to build metal cluster and ultra-small metal nanoparticle catalysts with promising performances for industrial applications. Clusters may not be the best structures in all reactions. We need to reveal some general rules that the size effect on different types of reactions using metal catalysts. It will be meaningful to compare the activities of single atoms, clusters and nanoparticles in typical reactions. The relative activity orders of single atoms, metal clusters and metal nanoparticles can be included, so that we can design corresponding catalysts according to such rules for specific reactions.

References

- [1] M. Stratakis and H. Garcia, *Chem. Rev.*, 2012, 112, 4469-4506.
- [2] M. Haruta, *Angew. Chem. Int. Ed.*, 2014, **53**, 52-56.
- [3] M. Haruta, *Gold Bull.*, 2004, **37**, 27-36.
- [4] M. Chen and D. W. Goodman, *Acc. Chem. Res.*, 2006, **39**, 739-746.
- [5] M. S. Chen and D. W. Goodman, *Science*, 2004, **306**, 252-255.
- [6] M. Valden, X. Lai and D. W. Goodman, *Science*, 1998, **281**, 1647-1650.
- [7] A. A. Herzing, C. J. Kiely, A. F. Carley, P. Landon and G. J. Hutchings, *Science*, 2008, **321**, 1331-1335.
- [8] C. C. Johansson Seechurn, M. O. Kitching, T. J. Colacot and V. Snieckus, *Angew. Chem. Int. Ed.*, 2012, **51**, 5062-5085.
- [9] A. Suzuki, *Angew. Chem. Int. Ed.*, 2011, **50**, 6722-6737.
- [10] J. Lindley, *Tetrahedron*, 1984, **40**, 1433-1456.
- [11] A. Klapars, J. C. Antilla, X. H. Huang and S. L. Buchwald, *J. Am. Chem. Soc.*, 2001, **123**, 7727-7729.
- [12] R. Hili and A. K. Yudin, *Nature Chem. Biol.*, 2006, **2**, 284-287.
- [13] M. Kidwai, V. Bansal, N. Kumar Mishra, A. Kumar and S. Mozumdar, *Synlett*, **2007**, 1581-1584.
- [14] M. J. Albaladejo, F. Alonso, Y. Moglie and M. Yus, *Eur. J. Org. Chem.*, **2012**, 3093-3104.
- [15] B. J. Borah, S. J. Borah, L. Saikia and D. K. Dutta, *Catal. Sci. Technol.*, 2014, **4**, 1047.
- [16] L. Rout, S. Jammi and T. Punniyamurthy, *Org. Lett.*, 2007, **9**, 3397-3399.
- [17] S. Jammi, S. Sakthivel, L. Rout, T. Mukherjee, S. Mandal, R. Mitra, P. Saha and T. Punniyamurthy, *J. Org. Chem.*, 2009, **74**, 1971-1976.
- [18] B.-X. Tang, S.-M. Guo, M.-B. Zhang, J.-H. Li, *Synthesis* 2008, 1707-1716.
- [19] S. Jammi, S. Krishnamoorthy, P. Saha, D. S. Kundu, S. Sakthivel, M.-A. Ali, R. Paul, T. Punniyamurthy, *Synlett* 2009, 3323-3327.
- [20] Y. Zijian, W. Xianwen, *Chin. J. Chem.* 2010, 28, 2260-2268.
- [21] B. Sreedhar, R. Arundhathi, P. L. Reddy and M. L. Kantam, *J. Org. Chem.*, 2009, **74**, 7951-7954.
- [22] P. Saha, T. Ramana, N. Purkait, M. A. Ali, R. Paul, T. Punniyamurthy, *J. Org. Chem.* 2009, **74**, 8719-8725.
- [23] M. L. Kantam, V. S. Jaya, M. J. Lakshmi, B. R. Reddy, B. M. Choudary, S. K. Bhargava, *Catal. Commun.* 2007, **8**, 1963-1968.

- [24] M. L. Kantam, V. S. Jaya, B. Sreedhar, M. M. Rao and B. M. Choudary, *J. Mol. Catal. A: Chem.*, 2006, **256**, 273-277.
- [25] H. C. Kolb, M. G. Finn and K. B. Sharpless, *Angew. Chem. Int. Ed.*, 2001, **40**, 2004-2021.
- [26] H. C. Kolb and K. B. Sharpless, *Drug Discovery Today*, 2003, **8**, 1128-1137.
- [27] H. Sharghi, R. Khalifeh and M. M. Doroodmand, *Adv. Syn. Catal.*, 2009, **351**, 207-218.
- [28] B. H. Lipshutz and B. R. Taft, *Angew. Chem. Int. Ed.*, 2006, **45**, 8235-8238.
- [29] S. Uk Son, I. Kyu Park, J. Park and T. Hyeon, *Chem. Commun.*, 2004, 778-779.
- [30] [B. S. Lee, M. Yi, S. Y. Chu, J. Y. Lee, H. R. Kwon, K. R. Lee, D. Kang, W. S. Kim, H. B. Lim, J. Lee, H. J. Youn, D. Y. Chi and N. H. Hur, *Chem. Commun.*, 2010, **46**, 3935-3937.
- [31] A. Kulkarni, R. J. Lobo-Lapidus and B. C. Gates, *Chem. Commun.*, 2010, **46**, 5997-6015.
- [32] M. Choi, Z. Wu and E. Iglesia, *J. Am. Chem. Soc.*, 2010, **132**, 9129-9137.
- [33] S. Goel, Z. Wu, S. I. Zones and E. Iglesia, *J. Am. Chem. Soc.*, 2012, **134**, 17688-17695.
- [34] C. Aydin, J. Lu, M. Shirai, N. D. Browning and B. C. Gates, *ACS Catal.*, 2011, **1**, 1613-1620.
- [35] E. Bayram, J. Lu, C. Aydin, A. Uzun, N. D. Browning, B. C. Gates and R. G. Finke, *ACS Catal.*, 2012, **2**, 1947-1957.
- [36] H. R. Moon, D. W. Lim and M. P. Suh, *Chem. Soc. Rev.*, 2013, **42**, 1807-1824.
- [37] A. Dhakshinamoorthy and H. Garcia, *Chem. Soc. Rev.*, 2012, **41**, 5262-5284.
- [38] D. Esken, S. Turner, O. I. Lebedev, G. Van Tendeloo and R. A. Fischer, *Chem. Mater.*, 2010, **22**, 6393-6401.
- [39] H. L. Jiang, Q. P. Lin, T. Akita, B. Liu, H. Ohashi, H. Oji, T. Honma, T. Takei, M. Haruta and Q. Xu, *Chem. Eur. J.*, 2011, **17**, 78-81.
- [40] J. Hermannsdorfer, M. Friedrich, N. Miyajima, R. Q. Albuquerque, S. Kummel and R. Kempe, *Angew. Chem. Int. Ed.*, 2012, **51**, 11473-11477.
- [41] H. L. Jiang, T. Akita, T. Ishida, M. Haruta and Q. Xu, *J. Am. Chem. Soc.*, 2011, **133**, 1304-1306.
- [42] X. Gu, Z. H. Lu, H. L. Jiang, T. Akita and Q. Xu, *J. Am. Chem. Soc.*, 2011, **133**, 11822-11825.
- [43] C. Wang, K. E. deKrafft and W. Lin, *J. Am. Chem. Soc.*, 2012, **134**, 7211-7214.
- [44] U. Diaz, *ISRN Chem. Eng.*, 2012, doi: 10.5402/2012/537164.
- [45] S. H. Joo, J. Y. Park, C. K. Tsung, Y. Yamada, P. Yang and G. A. Somorjai, *Nature Mater.*, 2009, **8**, 126-131.
- [46] S. Vajda, M. J. Pellin, J. P. Greeley, C. L. Marshall, L. A. Curtiss, G. A. Ballentine, J. W. Elam, S. Catillon-Mucherie, P. C. Redfern, F. Mehmood and P. Zapol, *Nature Mater.*, 2009, **8**, 213-216.